Laser micro-patterning
of dental zirconia:
effects on microstructure
and reliability

von

Erica Roitero

Saarbrücken

2018

Tag des Kolloquiums:	22 Februar 2018
Dekan:	Prof. Dr. Guido Kickelbick
Berichterstatter:	Prof. Dr.-Ing. Frank Mücklich
	Priv.-Doz. Dr.-Ing. Guido Falk
Weitere Mitglieder:	Prof. Diego Gomez
	Prof. Rosa Isabel Merino
	Prof. Emilio Jimenez-Piqué
Vorsitz:	Prof. Luis Llanes Pitarch

Zusammenfassnung

Tetragonales, polykristallines Zirkoniumdioxid, stabilisiert mit 3 Mol-% Yttriumoxid (3Y-TZP), ist eine beliebte Biokeramik für Dentalanwendungen, die aufgrund ihrer guten mechanischen Eigenschaften sowie Biokompatibilität und der erzielten ästhetischen Ergebnisse zunehmend Verwendung findet.

Es besteht ein wachsendes Interesse an der Modifizierung der Oberflächentopographie, um die biologische Reaktion auf diese Biomaterialien zu beeinflussen. Die Laserstrahlinterferenz (Direct Laser Interference Patterning, kurz: DLIP) erzeugt eine periodische Intensitätsverteilung, die das gewünschte Muster im Mikro- oder Nanometerbereich in die Oberfläche einbringt und das in einem einstufigen Prozess.

Das Ziel dieser Arbeit besteht darin zu verstehen, wie Nanosekunden-Laserinterferenzmuster die Topographie und Mikrostruktur von 3Y-TZP verändern und wie diese Veränderungen die Integrität und Zuverlässigkeit des Materials beeinflussen. Besonderes Augenmerk wurde auf die hydrothermale Abbaubeständigkeit nach der Laserstrukturierung gelegt, da diese Materialfamilie anfällig ist für Gefügeveränderungen durch Oberflächenbehandlungen.

Aufgrund von Thermoschock kommt es zu Mikrorissbildung, Rekristallisation, Restspannungen, Phasentransformationen und Texturierung werden auf der behandelten Oberfläche. Diese mikrostrukturellen Modifikationen sind hinsichtlich der mechanischen Integrität des behandelten Materials unbedenklich. Allerdings wird die LTD-Resistenz von 3Y-TZP durch eine derartige Laserbehandlung reduziert. Dementsprechend wird empfohlen durch eine anschliessende thermische Behandlung (bei 1200 ° C für 1 Stunde) langfristige Zuverlässigkeit.

Abstract

Tetragonal polycrystalline zirconia stabilized with 3% mol of yttria (3Y-TZP) is a popular bioceramic, increasingly used for dental applications thanks to its good mechanical properties, biocompatibility and aesthetic outcome.

There has been a growing interest in modifying the surface topography in order to influence the biological response to these biomaterials. Among the available methods, Direct Laser Interference Patterning (DLIP) allows patterning at the micrometric- and nanometric-scale in a single-step process. Its application to 3Y-TZP seems promising but needs a thorough characterization in order to ensure the short and long term stability.

Laser-material interaction mainly results in thermal effects, producing the desired topography alteration thanks to material melting and liquid flow. Pattern geometry and overall surface roughness can be modified independently varying laser fluence and number of pulses. Microcracking, recrystallization, residual stresses, phase transformation and texturization are produced on the treated surface due to thermal shock. These microstructural modifications are concentrated in a thin layer of material (1 μm thick) and are not a concern for mechanical integrity of the treated material. However, pre-existing defects on the surface can interact with the laser beam, becoming larger critical defects that lower the overall mechanical resistance. Low Temperature Degradation (LTD) resistance is reduced by the laser treatment because of the monoclinic phase and residual stresses induced by thermal shock.

To ensure the good outcome of such laser patterning on 3Y-TZP a thermal treatment (at 1200°C for 1 hour) is recommended to ensure the long term reliability.

Resumen

La circona poli-cristalina estabilizada con el 3% mol de yttria (3Y-TZP) es un material cerámico comúnmente utilizado en aplicaciones biomédicas y prótesis dentales gracias a sus buenas propiedades mecánicas, su biocompatibilidad y estética.

Hay un interés creciente en modificar la topografía de la superficie con el fin de influir en la respuesta biológica de estos biomateriales. Entre los métodos disponibles, el Patrón Láser Directo por Interferencia (*Direct Laser Interference Patterning*, DLIP) permite el modelado a escala micrométrica y nanométrica en un solo paso.

Este trabajo contribuye a comprender cómo el DLIP de nanosegundos modifica la topografía y la microestructura de 3Y-TZP y cómo estos cambios influyen en la integridad y fiabilidad del material después del tratamiento con láser. Se ha prestado especial atención a la resistencia a la degradación hidrotermal, debido a su susceptibilidad a los cambios microestructurales causados por los tratamientos de superficie.

La interacción del láser con el material produce principalmente efectos térmicos, creando la alteración de topografía deseada. Se producen microagrietamento, recristalización, tensiones residuales, transformación de fase y texturización en la superficie tratada debido al choque térmico. Estas modificaciones microestructurales se concentran en una capa superficial de material (1 μm de espesor) y no afectan la integridad mecánica del material tratado. La resistencia a la degradación hidrotermal se reduce mediante el tratamiento con láser. Un tratamiento de recocido es capaz de restablecer la resistencia a la degradación hidrotermal.

Preface

The work presented in this thesis is a result of my doctoral studies in the frame of the Erasmus Mundus European Joint Doctoral Programme in Material Science and Engineering (DocMASE). The project was developed among two universities, the Polytechnic University of Catalunya (UPC) and Saarland University (UDS), between November 2013 and November 2017. Two research groups were involved, the Center for Structural Integrity, Reliability and Micromechanics of Materials (CIEFMA) at UPC and the Functional Materials Group (FuWe) at UDS.

Erica Roitero

Barcelona, 2017

List of publications and author's contributions

I. **A parametric study of laser interference surface patterning of dental zirconia: effects of laser parameters on topography and surface quality.**
<u>E. Roitero</u>, F. Lasserre, M. Anglada, F. Mücklich, E. Jiménez-Piqué.
Dental Materials 33 (2017), e28–e38.
DOI: 10.1016/j.dental.2016.09.040

Author's contribution: Participation in the planning and design of the study. Sample preparation and experimental work. Analysis and discussion of results, in cooperation with the other co-authors. Manuscript writing.

II. **Nanosecond-laser patterning of 3Y-TZP: damage and microstructural changes.**
<u>E. Roitero</u>, F. Lasserre, J.J. Roa, M. Anglada, F. Mücklich, E. Jiménez-Piqué.
Journal of the European Ceramic Society 37 (2017), 4876–4887.
DOI: 10.1016/j.jeurceramsoc.2017.05.052

Author's contribution: Participation in the planning and design of the study. Sample preparation and experimental work, besides PED-TEM experiments. Analysis and discussion of results, in cooperation with the other co-authors. Manuscript writing.

III. **Low temperature degradation of laser patterned 3Y-TZP: enhancement of resistance after thermal treatment.**
<u>E. Roitero</u>, M. Ochoa, M. Anglada, F. Mücklich, E. Jiménez-Piqué.
Journal of the European Ceramic Society (2017) (article in press, accepted on 21/10/2017).
DOI: 10.1016/j.jeurceramsoc.2017.10.044

Author's contribution: Participation in the planning and design of the study. Sample preparation and experimental work, besides XRD experiments. Analysis and discussion of results, in cooperation with the other co-authors. Manuscript writing.

Furthermore, the following manuscript (to be submitted) is included as an annex for completeness:

IV.   **(ANNEX A) Mechanical reliability of laser patterned 3Y-TZP.**
E. Roitero, M. Anglada, F. Mücklich, E. Jiménez-Piqué.
To be submitted

Author's contribution: Participation in the planning and design of the study. Sample preparation and experimental work. Analysis and discussion of results, in cooperation with the other co-authors. Manuscript writing.

Contents

List of figures and tables

Glossary of terms

3Y-TZP: Tetragonal Polycrystalline Zirconia stabilized with 3 mol % of Y_2O_3

ATZ: Alumina-Toughened Zirconia

B3B: Ball-on-three-balls strength test

DLIP: Direct Laser Interference Patterning

EDX: Energy-Dispersive X-ray spectroscopy

FIB: Focused Ion Beam

LTD: Low Temperature Degradation

MAJ: Mehl-Avrami-Johnson

Nd:YAG: Neodymium-doped Yttrium Aluminum Garnet

PSZ: Partially Stabilized Zirconia

SEM: Scanning Electron Microscopy

TEM: Transmission Electron Microscopy

TZP: Tetragonal Polycrystalline Zirconia

WLI: White Light Interferometry

XPS: X-ray Photoelectron Spectroscopy

XRD: X-Ray Diffraction

Y-TZP: Tetragonal Polycrystalline Zirconia stabilized with Y_2O_3

ZTC: Zirconia Toughened Composite

ZTA: Zirconia Toughened Alumina

1. Introduction

1.1. Dental grade zirconia

1.1.1. Zirconia-based ceramics: an overview

Zirconium oxide (ZrO_2) presents the phenomenon of allotropy, forming monoclinic (*m*), tetragonal (*t*) and cubic (*c*) crystallographic structures as a function of temperature, at atmospheric pressure.
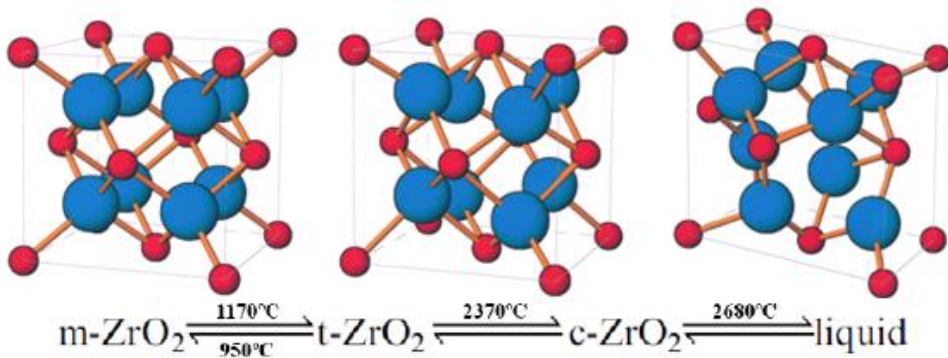
Fig. 1. Crystalline structures of zirconium oxide and their transition temperatures (reproduced from [1]*).*

The transformation tetragonal $\leftrightarrow$ monoclinic ($t \leftrightarrow m$) is martensitic and is accompanied by a volume variation of around 4-5%, if unconstrained [2,3]. Upon cooling the volume expansion may lead to severe cracking of the material, compromising the integrity and causing premature failure. For this reason, the large use of pure zirconium oxide as a technological material was prevented until 1920's when two groups discovered that tetragonal and cubic phases could be metastable at room temperature, avoiding catastrophic failure. Alloying zirconium oxide with other cubic oxides (named therefore "stabilizers") allows the high temperature phases to exist at room temperature.

However, only in 1975 Garvie *et al.* [4] discovered that the retention of the metastable *t*-phase and its release during crack propagation contribute to increase the fracture toughness of the material. During the propagation of a crack inside the material the metastable *t*-grains undergo stress-induced transformation. The volume increase associated to phase change of constrained grains induces a compressive field in the surrounding matrix that

hinders further crack propagation. This mechanism (also known as "transformation toughening") opened the way to the employment of zirconia-based ceramics in many engineering applications, thanks to the combination of high mechanical properties with low thermal conductivity, ionic conductivity and chemical stability. Typical applications are refractory and thermal-shock resistant parts, thermal barriers coatings and high-temperature ionic conductors, solid-oxide fuel cells, oxygen sensors and for biomedical devices.

However, the thermodynamic metastability of the t-phase is the origin of the main drawback of this material: Low Temperature Degradation (LTD, also known as "aging"). This is the spontaneous and progressive transformation of metastable t-zirconia grains to m-phase, triggered by water molecules that start from of the surface of the material exposed to humid environment at moderate temperatures. Aging results in surface roughening, micro-cracking and grain pull-out [5] and is therefore detrimental for material integrity and long-term reliability.

Independently from the stabilizer employed, three different types of engineering zirconia-based ceramics may be defined:
- Partially Stabilized Zirconia (PSZ): a matrix of c-phase embedding transformable t-phase precipitates.
- Zirconia Toughened Composites (ZTC): a matrix with high elastic modulus embedding transformable t-phase grains. The most used matrix is Alumina and the material is known as zirconia toughened alumina (ZTA)
- Tetragonal Zirconia Polycrystal (TZP): all the zirconia grains are constituted by transformable t-phase .

In this work the attention will be focused on the TZP family, since it is the most commonly employed in biomedical field [6].

1.1.2. Yttria stabilized Zirconia (YSZ)

The most studied stabilizers oxides for biomaterials applications are CaO, MgO, Y_2O_3 and CeO_2 [2]. However, only ZrO_2-Y_2O_3 system reached the actual status of having a dedicated ISO standard for surgical application (ISO 13365 [6]) due to its optimal combination of fracture toughness and strength, as schematized in Fig. 2.
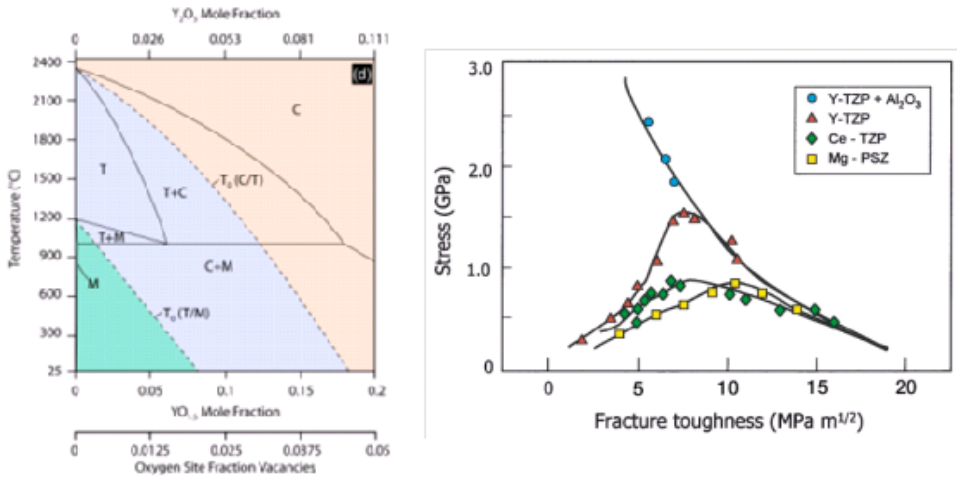
Fig. 2. On the left, phase diagram of Y2O3-ZrO2 system, with the stability and metastability regions (reproduced from [7]). On the right, fracture toughness versus strength of different zirconia-based ceramics (reproduced from [8]).

The introduction of Y_2O_3 in the ZrO_2 lattice gives origin to oxygen vacancies because of charge compensation [7]:

$$Y_2O_3 \overset{ZrO_2}{\longleftrightarrow} 2\,Y'_{Zr} + 3\,O^x_O + V^{\cdot\cdot}_O \tag{1}$$

The lower valence and oversized cations Y^{3+} substituting the Zr^{4+} cations in the lattice structure generate both oxygen vacancies and a dilatation of cation network. These favor a sevenfold coordination of oxygen anions around Zr^{4+} and induce crystal distortions capable of relieving the oxygen overcrowding around the small cation Zr^{4+} (the latter being at the origin of the poor stability of undoped tetragonal phase at low temperatures [7]). Typically 3 mol% and 8 mol% of Y_2O_3 in ZrO_2 are used to retain down to room temperature the tetragonal and the cubic form, respectively. The portion of phase diagram reported in Fig. 2 indicates the most agreed upon stability and metastability regions for low Yttria contents as a function of temperature. Most attractive compositions for transformation toughening are those with low Yttria concentration (typically 2-3%), able to retain metastable *t*-phase but also high enough to prevent spontaneous $t \rightarrow m$ transformation upon cooling [7].

The amount of dopant is not the only variable influencing phase stabilization when considering a more realistic polycrystalline solid, where a grain is mechanically constrained by the surrounding matrix. In this case, the reaction forces exerted by the surrounding matrix and the interfaces play a

role. From a thermodynamical point of view this can be addresses taking into account the different contributions to the change of total free energy for the $t \rightarrow m$ transformation ($\Delta G_{t \rightarrow m}$) of a t-phase grain (or particle) embedded in an infinite matrix:

$$\Delta G_{t \rightarrow m} = \Delta G_C + \Delta G_{SE} + \Delta G_S \qquad\qquad (2)$$

The chemical free energy contribution (ΔG_C) depends on temperature and stabilizers concentration. The elastic strain energy contribution (ΔG_{SE}) depends on surrounding matrix stiffness, size and shape of particles, the presence of internal or external stresses. The surface contribution (ΔG_s) is associated to the formation of new interfaces. Phase transformation occurs if $\Delta G_{t \rightarrow m} \leq 0$ and therefore depends on all the above mentioned parameters.

The ability of metastable t-grains to transform to m-phase upon the application of a stress is the reason for the high toughness of this family of ceramics. The energetic approach (2) also helps to understand the driving forces of the stress-activated transformation [8]. The free energy barrier between the metastable t-phase and the m-phase may be overcome by the energy provided by the applied stress (strain). When the strain is induced by the stress field at the tip of a crack, the transformation of the constrained t-phase grains will generate compressive forces inside the untransformed matrix. As the crack advances, the transformed volume reaches the crack wake and the residual compressive stress hinder further opening.
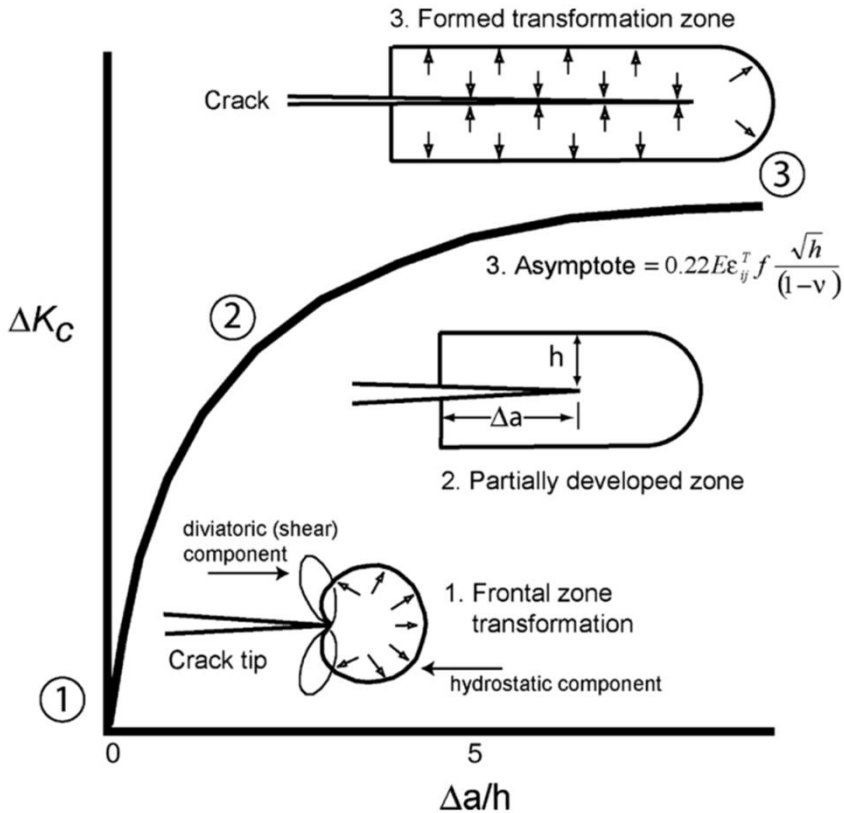
Fig. 3. Schematic representation of the transformation zone development and fracture toughness increment (ΔKc) with crack extension (Δa/h) (reproduced from [8] *from an adaptation from*[9]*) .*

The increment in toughness is dependent on the ease of transformation and therefore depends on the parameters governing the stability of the *t*-phase. To sum up, these parameters and their effect on *t*-phase stabilization and toughening are:
- amount and distribution (homogeneity) of dopant ions: the higher ;
- amount of retained *c*-phase: being more rich in Yttria, the presence of this phase can cause a depletion of stabilizer content in the surrounding grains, making them more transformable;
- grain size: for a given dopant concentration, the toughness increment decreases as grains become much smaller than the critical size, presumably due to "over-stabilization" of the grains, eliminating the $t \rightarrow m$ transformation upon introduction of a crack;
- density and porosity;

- residual stresses: tensile residual stresses can lower the nucleation stress threshold for the $t \rightarrow m$ in the presence of crack-tip strain energy while compressive residual stresses can help stabilizing the t-phase.

All the above mentioned characteristics determine the mechanical properties but also the resistance to LTD of the material. Unfortunately, the Y-TZP compositions that show the best performances for the fracture toughness are at the same time those that are the most susceptible to LTD [7]. This happens because the transformability of the tetragonal phase, which promotes transformation toughening, is in general also responsible for the driving force for LTD. These aspects will be discussed further in *1.1.3* and *1.1.4*.

1.1.3. Low Temperature Degradation: an issue for biomedical applications

In 3Y-TZP, LTD consists of a $t \rightarrow m$ transformation at the sample surface in a humid atmosphere, followed by integrity loss of the surface and eventual reduction of mechanical properties after very long degradation time [5]. These negative consequences are due to surface roughening, microcracking and grain pull-out caused by the volume increase associated to phase transformation.

Aging starts at the surface in contact with water molecules and then propagates towards the bulk of the material. The role of water molecules in the destabilization of t-phase is still not completely understood, however, the majority of reports [2,5,10–14] agree that the penetration and diffusion of water-derived species inside the crystal lattice reduce the number of oxygen vacancies and introduce internal stresses in the crystal lattice modifying the local oxygen configuration around Zr^{4+} [7]. There is still an open debate about the nature and diffusion mechanism of the water-derived species responsible of the destabilization. At first it was proposed that hydroxyls [12] or water molecules [13] diffuse inside the lattice by an oxygen vacancy diffusion mechanism, as schematized in Fig. 4. However, T. Duong *et al.* have demonstrated in [14] that water-derived species are more likely to be H^+ and O^{2-} diffusing in a parallel but independent way within oxygen vacancy sites.
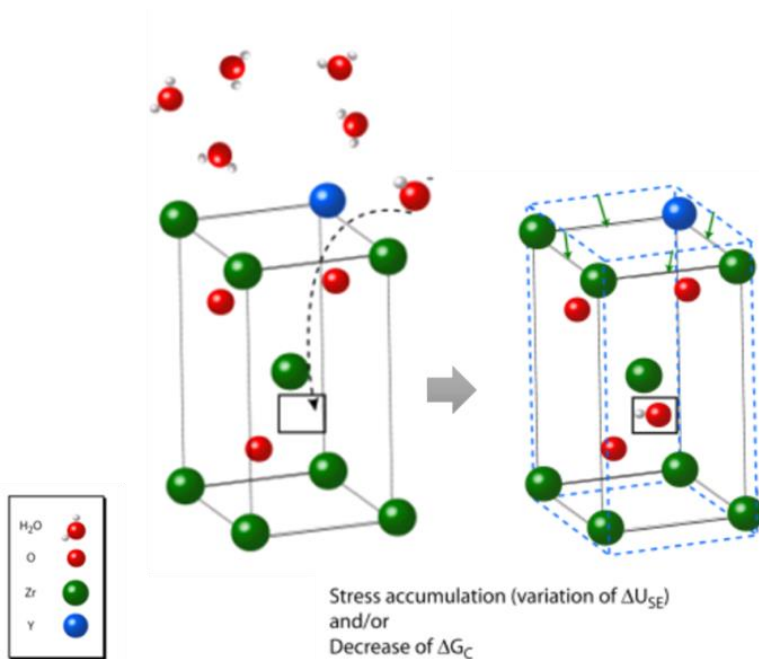
Fig. 4. One of the proposed mechanisms involved in the destabilization of the t-phase (reproduced from [7]).

The kinetics of LTD has also been a debated topic: authors agree that on the surface in contact with water the transformation of the metastable *t*-phase to *m*-phase can be well described by a "nucleation and growth" mechanism [5,15]. The first isolated nuclei form mainly at grain boundaries, where water-derived species diffusion and *t*-phase destabilization are easier because of higher crystalline disorder. The nuclei of *m*-phase then start to grow and spread on the surface, until reaching saturation, and then the transformation front proceeds towards the bulk (Fig. 5).
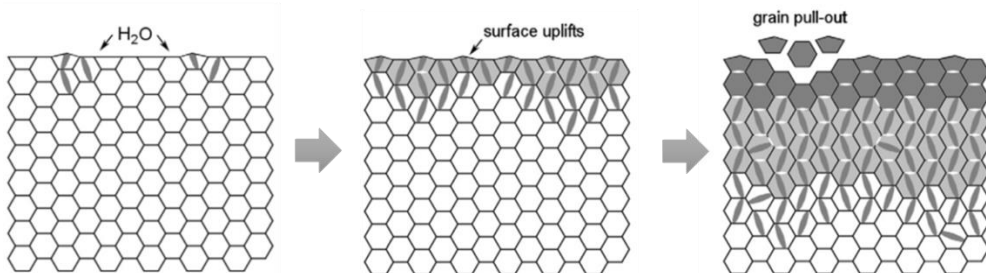
Fig. 5. Sketch of the propagation of the transformation inside the material (adapted from [16]).

The first *m*-phase nuclei are in the form of martensite plates inside untransformed grains and generate local shear tension in the surrounding *t*-

phase grain and at the grain boundary with untransformed adjacent grains. Phase transformation within a single grain is then propagated by self-accommodating variants (twinning). On the unconstrained free surface strain is easily accommodated by surface uplifts. Local stresses at the grain boundary can nucleate microcracks and induce $t \rightarrow m$ transformation in the neighboring grains, activating the so-called "autocatalytic propagation" [16]. The latter is nowadays the most recognized mechanism of propagation for LTD inside the bulk of the material [16–18]: the local stresses accumulated at the degradation front are considered the driving force for further transformation.
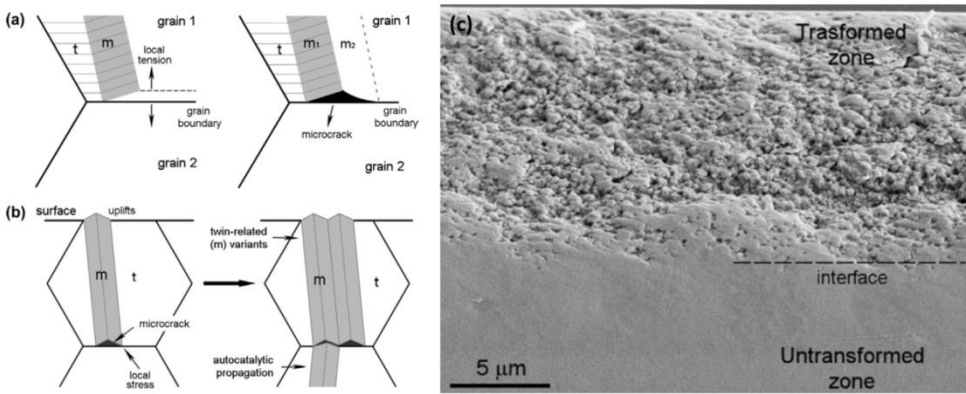
Fig. 6. On the left, schematization of $t \rightarrow m$ transformation within a single grain (a) and inside neighboring grains (b). On the right, a cross section of degraded 3Y-TZP: the transformed layer has lost integrity due to microcracking and grains pull out (adapted from [16]).

Experimentally, the kinetics of LTD has been described by plotting the volume fraction of m-phase as a function of time [5], resulting in sigmoidal-shaped curves that can be well fitted with Mehl-Avrami-Johnson (MAJ) equation describing time-dependent isothermal phase transitions:

$$V_m = V_{m\ min} + (V_{m\ max} - V_{m\ min})[1 - \exp(-(bt)^n)] \qquad (3)$$

where $V_{m\ min}$ is the minimum and initial monoclinic volume fraction, $V_{m\ max}$ is the maximum monoclinic volume fraction reached, b and n are adjustable parameters (b depends temperature and is related to the activation energy of the process while n is a constant also known as MAJ exponent) and t is the aging time [19].
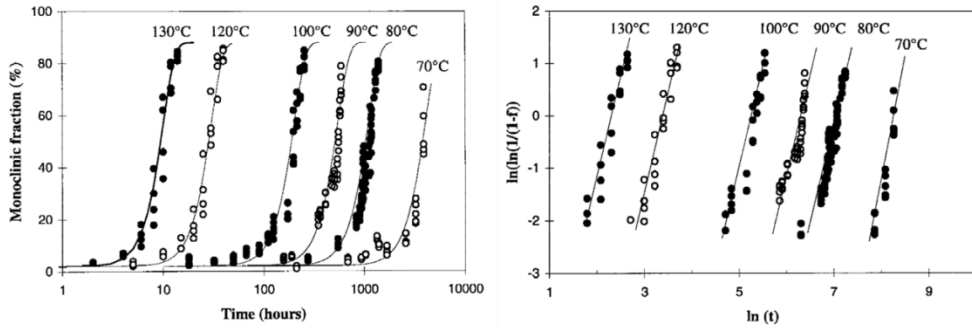
Fig. 7. LTD kinetics curves for 3Y-TZP at different temperatures. On the left, the monoclinic volume fraction is plotted as a function of time. On the right, the same quantities are plotted in logarithmic scale for the determination of parameters n and b of the MAJ equation (reproduced from [5]).

Microstructural and compositional alterations due to mechanical or thermal modifications change the LTD kinetics of 3Y-TZP. The parameters *b* and *n* calculated from the fitting with MAJ equation for the modified material therefore deviate from those calculated for the untreated zirconia [20,21].
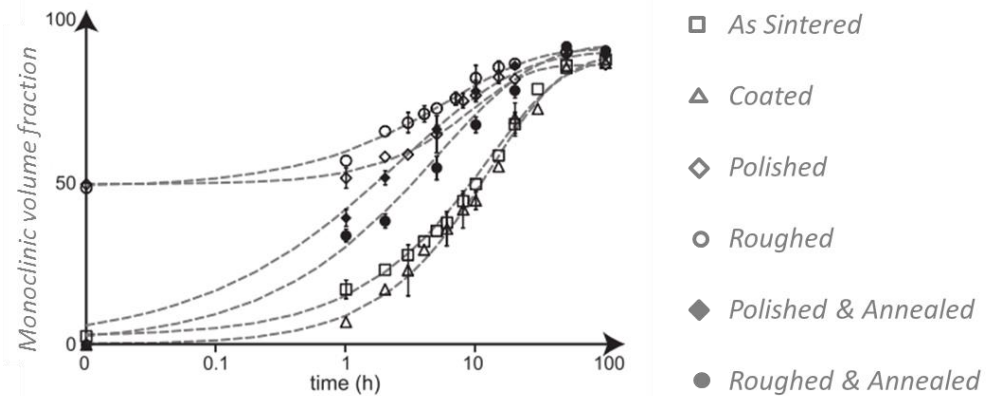
Fig. 8. LTD kinetics curves of 3Y-TZP modified with different surface treatments: acceleration and deceleration of the kinetics result from microstructural modifications induced by different treatments (adapted from [20]).

The shape of the MAJ equation is sigmoidal and, in the field of $t \to m$ transformation and aging, it has had a considerable success since it allows an extrapolation of the times required for aging at low temperatures from data collected at high temperatures, which are much faster to acquire (accelerated LTD tests) [2]. It is of paramount importance to apply this equation with due awareness of its validity limits and significance: extrapolation of aging times at room temperature from higher temperature tests requires the accurate

determination of parameters b and n, which strongly vary with composition and microstructure. This extrapolation can be done correctly only repeating the accelerated tests at least at two different temperatures for each type of zirconia, otherwise the use of approximations can result in severe overestimations (or underestimations) of life time at room temperature [2].

The above described method of determining the kinetics of LTD for t-phase zirconia ceramics is generally applied on monoclinic volume fraction data calculated with Toraya method [22,23] from datasets acquired with X-Ray Diffraction (XRD) [5]. Limits of this technique are the finite penetration depth of X-Rays, restricting the analysis to the first µm below the surface, and their attenuation with absorption depth, that may originate underestimations due to the inhomogeneous signal coming from the analyzed volume. Lately, other experimental techniques have been employed to describe the propagation of $t \rightarrow m$ transformation towards the bulk of the material, like Raman Spectroscopy and Scanning Electron Microscopy (SEM) on cross sections. This different approach has allowed the determination of the thickness of the transformed layer as a function of time instead of the monoclinic volume fraction. This in turn allowed the proposition of a linear kinetics [17,18] of the transformation instead of a sigmoidal, which is still a topic of debate among researchers.

LTD has a paramount importance in biomedical applications because of the exposure of these materials to physiological environment. However, it has not always been taken adequately into account [3] and it has unfortunately been at the origin of unexpected failures in orthopedic applications [24]. In 2001, firms distributing zirconia started recalling femoral heads owing to a series of premature fractures. The origin of failures was related to an accelerated LTD of zirconia due to a change in the production process, in a limited number of batches of implants. Although the cause of failure was well identified, it brought to an end the use of zirconia as hip replacement, despite its superior properties compared to other materials. This failure episode emphasized the critical role of LTD on zirconia implants: several clinical studies and retrieval analyses showed that even zirconia implants processed under the best conditions could suffer from a certain degree of degradation in vivo [7].

Nevertheless, the application of 3Y-TZP in orthopedics in the 1990s encouraged its development for dental restoration components such as crowns and bridges. The material can be expected to be as susceptible to LTD as in orthopedic applications, even though the temperatures are somewhat lower. Although the consequences of failure of a dental implant or dental

restoration device is less critical to a patient than that of an orthopedic implant, the durability of these dental devices is expected to be no less of an issue for their manufacturers [7]. The future of this material in dental applications depends strongly on the careful consideration of this weak point of the material.

1.1.4. 3Y-TZP as a bioceramic

Its physical, mechanical (i.e. high strength, hardness, wear resistance, resistance to corrosion, and elevated fracture toughness) and chemical properties make zirconia a material of interest for biomedical sciences. As can be observed in the following table, biomedical grade Y-TZP exhibits excellent mechanical properties among single phase oxide ceramics. Its higher toughness makes it preferable to more brittle alumina-based materials for many structural applications as a bioceramic, even if its compressive strength and hardness are lower (see Fig. 9).

	Alumina	*Mg-PSZ*	*TZP*
Chemical components	*99.9 % Al_2O_3*	*ZrO_2 + 8 - 10 mol % MgO*	*ZrO_2 + 3 mol% Y_2O_3*
Density [g cm^{-1}]	*≥ 3.97*	*5.74 - 6*	*> 6*
Porosity [%]	*< 0.1*	*-*	*< 0.1*
Bending strength [MPa]	*> 500*	*450 - 700*	*900 − 1200*
Compression strength [MPa]	*4100*	*2000*	*2000*
Young modulus [GPa]	*380*	*200*	*210*
Fracture toughness [MPa m$^{1/2}$]	*4*	*7 - 15*	*7 − 10*
Thermal expansion coefficient [K^{-1}]	*$8 \cdot 10^{-6}$*	*$7 -10 \cdot 10^{-6}$*	*$11 \cdot 10^{-6}$*
Thermal conductivity [W m K^{-1}]	*30*	*2*	*2*
Hardness [HV 0.1]	*2200*	*1200*	*1200*

Fig. 9. Comparison of some properties of bioceramics materials (adapted from [25]).

The first reference concerning its application in medicine appeared in the late Sixties followed twenty years later by the first publication referring to its use in orthopedic surgery and particularly in total hip replacement.

However, it is only in the early nineties that zirconia found its application in dental prosthetic surgery [11].

Today, there is a trend in dental implantology to develop new ceramic-based implants for their enhanced capacities of peri-integration, osseointegration, reduction of plaque accumulation leading to an improvement of the soft tissue management, and aesthetic consideration, as an alternative to monolithic titanium implants[11]. Although many types of zirconia-containing ceramic are currently available, only three are used to date in dentistry[26] Y-TZP, Mg-PSZ and ZTA, This work will focus only on ZrO_2 stabilized with 3% molar Y_2O_3 and the following discussion will be centered mainly on this system.

1.2. Surface modification and micropatterning with laser techniques

1.2.1. The surface of biomaterials

The interface zone between an implant and the surrounding tissue is the most important entity in defining the biological response to the implant and the response of the implant to the body [27].

In order to understand what happens at the surface of an implant when it is placed in contact with a physiological environment, it is necessary to identify which species are present and which are the possible interactions with the material surface. Biological systems in contact with a surface include: water, water and hydrated ions, amino acids, nucleic acids, lipids, lipid membranes, peptides, saccharides, polysaccharides, vesicles, liposomes, proteins, DNA, supramolecular complexes, cells and organized living tissue [28]. Water is the first species to come in contact with the surface and then small inorganic and organic molecules may be adsorbed onto the surface (specifically or not, depending on the physic-chemical characteristics of the surface). Bigger entities, like bacterias and human cells, reach the surface later and their adhesion is strongly mediated by the adsorbed film on the surface of the implant.

The success of the implant (that may be seen as the lack of negative reaction of the body to the introduction of a foreign material) depends on the bacterial colonization versus the tissue adhesion to its surface. In the paper by G. Gristina [29] it is suggested that the fate of an available surface may be conceptualized as a "race for the surface", which is a contest between tissue

cell integration and bacterial adhesion to that same surface. If the competition is won by bacterias, tissue cells will not be able to subsequently colonize the surface and the success of the implant would be compromised. Even if tissue cells succeed in spreading over the surface, still remains the risk of being displaced by bacterias with the consequent failure of the implant. The biological mechanisms and sequences of reactions are still far from being completely clarified and categorized.
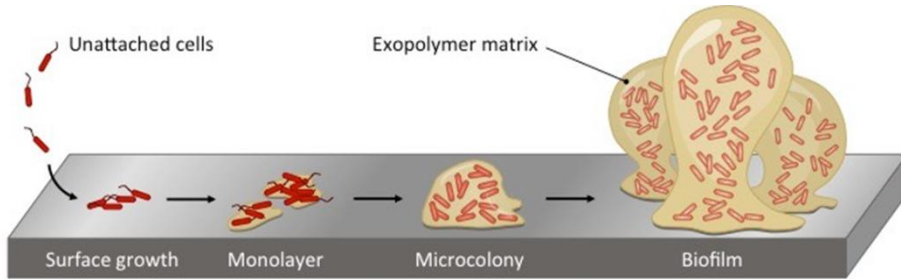
Fig. 10. Formation steps of a biofilm.

When describing the behavior of bacteria it is important not to forget that they are an entire ecosystem: the cells alone cannot survive and, since they need to provide nutrients and to dispose of byproducts, they tend to organize into complex structures that facilitate their survival, called colonies. A colony is composed of the microorganisms together with the extracellular organic molecules (secreted polymers like saccharides, proteins and glycoproteins). When these microorganisms organize themselves onto a surface, the structure is called biofilm (see Fig.10). The forces that mediate bacterial adhesion to surfaces have been reasonably well identified and include ubiquitously present attractive Van der Waals forces, electrostatic interactions, and acid-base bonding [30]. The survival of the biofilm on a surface is the result of the equilibrium between these adhesion forces and external forces that promote its break-up.

It is of paramount importance to identify the surface characteristics that influence biofilm formation and adhesion on implant surfaces. Many studies [30–38] have been performed to determine the influence of surface characteristics on bacterial adhesion. Generally, it is agreed that the most effective are surface free energy (low surface free energy disfavor bacterial adhesion) and roughness (smoother surfaces reduce bacterial adhesion). The majority of the authors also agree about the predominant effect of roughness on surface free energy. However, a smoothening below a Ra=0.2 µm showed no further significant changes and this value was therefore suggested as a

threshold surface roughness, below which bacterial adhesion cannot be further reduced [31]. These general considerations have been drawn for titanium, however, they have been extended to zirconia by many research groups [32–35,38–40]. On the other hand, in one of the latest reviews about dental materials with antibiofilm properties when dealing with ceramic materials Wang *et al.* [38] conclude that "the increase in roughness did not significantly facilitate biofilm formation. Apparently, low biofilm accumulation makes ceramic a promising material for various indications". It is clear that the topic is far from being satisfactorily understood and there are no unambiguous reference values that allow an identification of the ideal antibiofilm roughness for zirconia surfaces. Furthermore, in the majority of the studies [32–35,38–40]the roughness is usually characterized by only one bidimensional parameter or maximum two, while other authors [41] suggest the use of more than one tridimensional parameters to characterize satisfactorily the topography and roughness.

Biofilms form on most surfaces exposed to the natural environment, including the human mouth. Biofilms on ceramics are thin and highly viable. Compositional and microstructural differences between different ceramics may, however, influence the surface properties and hence the reactions between the material and oral microbial environment. Biofilm formation on various types of dental ceramics (e.g. veneering glass–ceramic, lithium disilicate glass–ceramic, yttrium-stabilized zirconia) for different purposes differs significantly. In particular, zirconia ceramic exhibits low plaque accumulation, and displays similar bacterial binding properties to titanium [38].

1.2.2. Surface modification and functionalization of biomaterials

Surface functionalization has become of paramount importance and is considered a fundamental tool for the development and design of countless devices and engineered systems for key technological areas in biomedical, biotechnological and environmental applications [42]. Over the years, many surface functionalization strategies have been developed and optimized. They can be divided into three main categories: physical, chemical and biological.
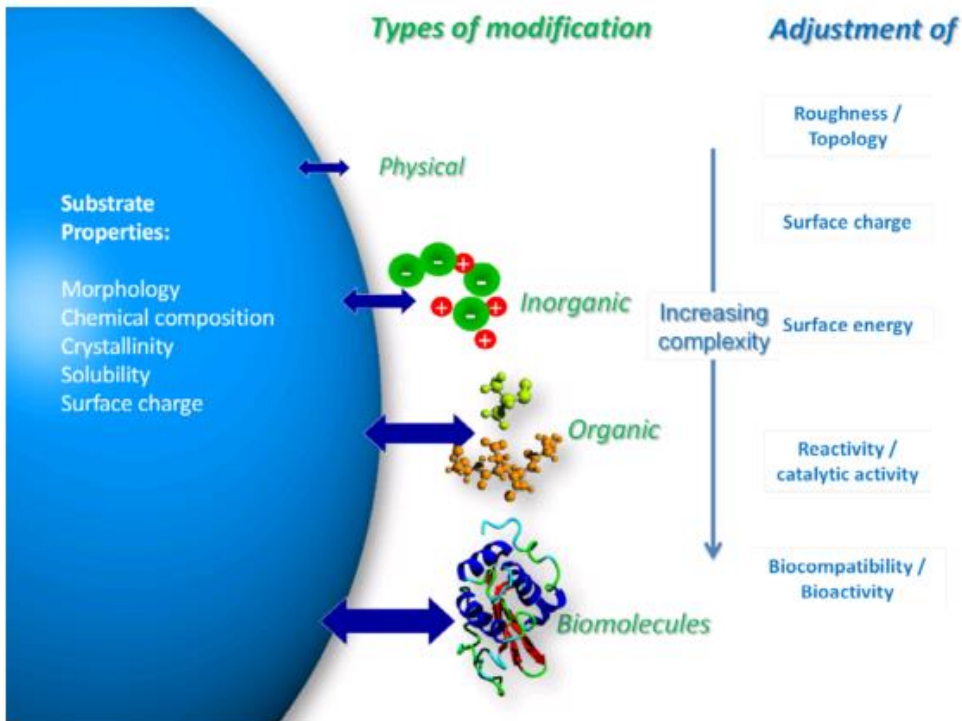
Fig. 11. Functionalization strategies for biomaterials (reproduced from [42]*).*

In this thesis the attention is focused on physical functionalization aimed at modifying and tuning the topography and the roughness of zirconia-based ceramic surfaces, at micrometric and submicrometric scale for biomedical applications.

Among the physical surface modification methods available for ceramics the most common can be identified as machine-aided approaches, polishing, grinding, sandblasting, acid etching and laser treatment. These techniques have been widely utilized in an attempt to enhance adhesion to different synthetic substrates or medical implant integration, and are thus highly attractive for tissue engineering applications or for the spatial control of cells on materials [42]. In fact, the fabrication of defined micropatterns smaller than 100μm in ceramics is still very challenging due to their high hardness and low brittleness. M. Holthaus *et al.* [43] performed a comparative study of different techniques to pattern the surface of ceramics materials such as alumina, zirconia, silica and hydroxyapatite. In this study the following techniques were tested: stamping with microtransfer molding, aerosol-jet® printing, computer-numerical-control machining and direct

laser interference patterning. They conclude that "laser treatment processes have high costs for technical equipment, but the production time is low. Especially direct laser interference patterning (DLIP) offers a fast and accurate patterning of ceramic surfaces". Laser is therefore considered a valid technique for local modification and patterning of surfaces (for metals, polymers and ceramics). It allows the creation of defined features at the micrometric scale, allowing the production of complex geometries and periodic patterns at the scale size of biological entities. Furthermore, it is a contactless technique, a particularly interesting aspect for biomedical applications since it strongly reduces surface contamination. Even if it is slightly more expensive when compared to other physical functionalization techniques, it is very fast and highly reproducible, making it very interesting from an industrial point of view.

In this work, DLIP will be exploited to texture the surface of 3Y-TZP. In order to understand how the technique works and how the modifications of the material are obtained, a brief overview about laser based techniques is given in the following paragraphs 1.2.3 and 1.2.4.

1.2.3. Laser techniques: an overview

The term laser stands for Light Amplification by Stimulated Emission of Radiation [44]. The main difference from other light sources is that it can emit coherent electromagnetic radiation. Spatial coherence means low divergence, which implies that the beam may be focused into a very tiny spot and that the beam remains collimated over a large distance. Temporal coherence means that the emitted radiation is almost monochromatic.

The main laser parameters to take into account are:
- wavelength (λ);
- power;
- intensity (I) and fluence (energy per unit surface, F), with their time and space distribution and mean values;
- pulse duration (τ), if it is a pulsed laser source;
- polarization.

The laser beam can be well represented by a monochromatic linearly polarized plane electromagnetic wave, propagating in time (t) and space (along x-direction). The electric and magnetic field it is carrying (E, H) may be described by a harmonic wave oscillating in a perpendicular direction to the propagation direction:

$$E = E_0\, e^{i\left(\frac{2\pi x}{\lambda}-\omega t\right)} \hspace{4cm} (4)$$

where λ is the wavelength and ω is the angular frequency.

Lasers find application in many different fields, from laboratory to industrial equipment to everyday-life devices. Depending on the wavelength and intensity of the emitted radiation, different interactions with materials may arise and may be exploited for completely different purposes. Low-energy interactions, that do not alter material properties, may be used as a source of information (spectroscopic techniques like Raman Spectroscopy). Higher-energy interactions, that lead to material modifications like phase or compositional changes, may be exploited as a mean to machine and modify materials (cutting, drilling and welding of metals or surface patterning). Thanks to lasers, thermal and chemical treatment of materials can be strongly localized, thereby leaving the substrate almost unaffected. Consequently, the laser technique allows one to process heat-sensitive materials better than other techniques requiring thermal treatment of the whole material (see Chemical Vapor Deposition as an example). In Fig. 12, different applications of lasers are mapped as a function of pulse duration and absorbed power.
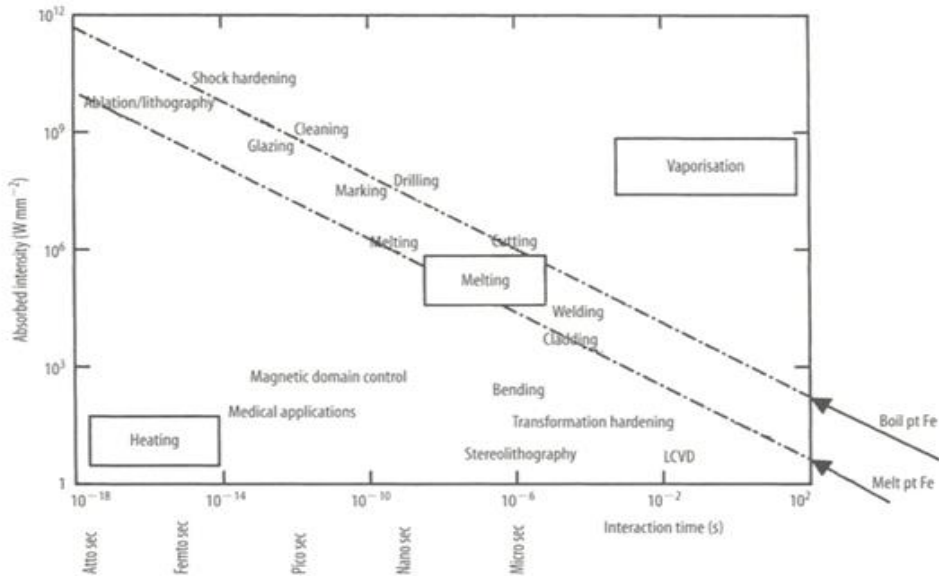
Fig. 12 Laser applications for steel machining. Techniques and physical mechanisms allowing material modifications are listed depending on the temporal mode regime (reproduced from [45]).

Lasers may be considered as electromagnetic energy sources characterized by many different parameters like wavelength, power, pulse duration. They can be categorized [46] depending on:

- emitted wavelength: the spectrum interesting for most technological applications is from infrared to ultraviolet, although lower and higher may be used;
- temporal mode: the emission may be continuous over time (Continuous Wave) or intermittent (Pulsed), with pulses duration down to the femtosecond regime;
- emitted power.

In Fig. 13Fig. 13. At the top, laser sources with the emitted wavelength, the regime (continuous or pulsed) and the emitted power (reproduced from *[47]*). At the bottom, the same sources and their technological application (adapted from*[46]*). are listed some laser sources with their characteristics.
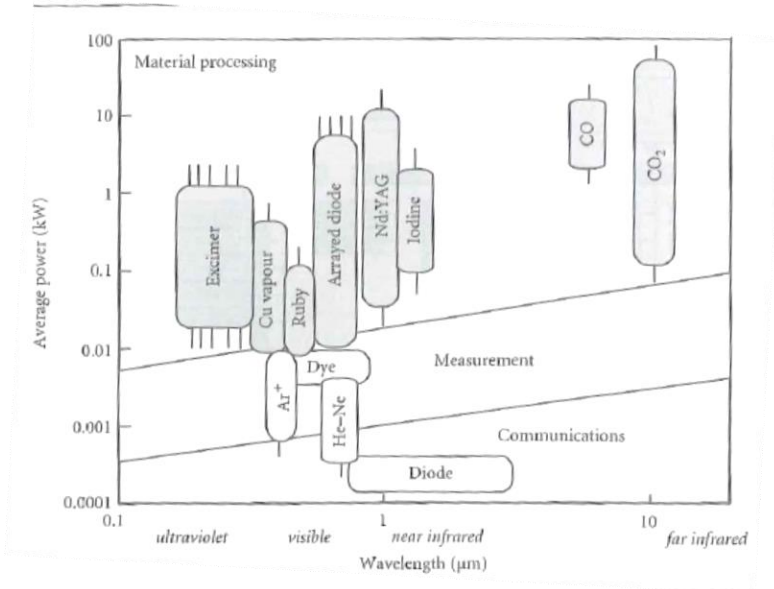
Laser type	Description	Average power [W]	Efficiency [%]
Excimer	248 nm - pulsed	100	2 – 4
YAG	355 nm – pulsed	10	0.1
YAG	266 nm – pulsed	3	< 0.1
N_2	377 nm – pulsed	1	< 0.1
Ar^+	330 – 360 nm - cw	7	< 0.01
Ar^+	275 – 305 nm - cw	0.5	< 0.01
He-Cd	325 nm - cw	0.01	0.1
Au	320 nm – pulsed	1.5	0.1

Fig. 13. At the top, laser sources with the emitted wavelength, the regime (continuous or pulsed) and the emitted power (reproduced from [47]*). At the bottom, the same sources and their technological application (adapted from*[46]*).*

In order to be able to design the parameters for a specific application it is important to understand the processes behind laser-matter interaction, since these are the origin of material modification. For a given substance, laser parameters have to be carefully selected to attain a specific regime and mechanism of interaction.

1.2.3.1. Laser interaction with matter

The interaction of the laser beam with matter involves the interaction of its photons with the fundamental constituents of the material (molecules, atoms and subatomic particles). In a solid crystalline material, the oscillating electric and magnetic fields of the incident electromagnetic wave mainly interacts with the lightest charged species, i.e. electrons. As any other electromagnetic radiation also laser beam may be partly reflected, absorbed and transmitted through a medium, depending on the electronic response of the material.

Laser-beam interaction with matter may produce very different phenomena, depending both on laser parameters and material properties. Laser parameters that influence the most this interaction are pulse duration (*i.e.* interaction time), wavelength and fluence. From the material point of view, both optical and thermal properties determine its response to laser illumination.

The incident radiation will perturb mainly electrons, bond or free, and will initiate a forced vibration against their lattice-counterpart [45]. The interaction may be schematized in two subsequent processes:
- energy absorption;
- energy conversion (or relaxation).

The first step involves the mechanisms by which a material absorbs the energy of the incident radiation and the second involves the mechanisms by which it transforms and redistributes this absorbed energy, within its absorption depth and the surrounding volume [47].

1.2.3.2. Laser energy absorption

In order to clarify the absorption phenomenon, materials may be classified according to their electronic structure and optical properties in metals and non-metals (further divided into semiconductors and dielectrics)

[48]. Incident laser electromagnetic field induces oscillation of charged species, i.e. electrons, into the material. Then, depending on the electronic structure of the material and the intensity and wavelength of the incident radiation, the latter may be re-emitted (scattered) or absorbed. For absorption to take place, electron oscillation should be transformed into an energy gain of the system, i.e. an excited state. Intra-band transitions are typical of electron excitations in metals while inter-band transitions and electron excitation from valence to conduction band are important in non-metals [49].

Metals behavior is governed by their free (conduction) electrons: incident laser photons are absorbed by these species, promoting them up to excited states. Incident laser-beam makes these electrons oscillate according to its electromagnetic field. Subsequent collision of these electrons with other species (i.e. other electrons and lattice ions) converts this oscillation in kinetic energy of the electron [49]. These excited states exist at some density and lifetimes and subsequently convert stored photon energy into other forms of energy, mainly heat (*i.e.* phonons) in metals [47].

Non-metals have mainly bound electrons and are basically transparent [48]. Their electronic states may be divided into a valence and a conduction band: in the absence of excitation and at standard conditions, the lower valence band is populated by bound electrons and few free electrons occupy the conduction band. If the incoming photon has enough energy it may provoke an inter-band jump, otherwise other indirect mechanisms may promote electronic excitation.

For direct photon absorption to happen, the incident photon must have and energy at least equal to the band gap (E_g) energy of the material. However, at high laser beam intensities, multi-photon absorption may occur and the inter-band transition may be achieved thanks to the cooperation of two or more photons with energy lower than the band gap. Semiconductors have band gaps of up to a few eV (visible and UV field) and dielectrics possess band gaps in the order of 5-10 eV (UV and deep UV field) [47].

In the case of photon energy lower than the band gap, the incident radiation makes electrons oscillate against their positive counterpart (lattice ions) producing a macroscopic polarization of the material. By subsequent collisions the few free electrons may gain enough net kinetic energy to promote excitation of a valence electron to a conduction band state. Electron-hole pairs are created or, from another perspective, ionization takes place. This process may lead to an avalanche of ionization events, as the number of

free carriers increases. This transformation may also be seen as a conversion of a non-metal to a metal-like state.

1.2.3.3. Relaxation processes

Regardless the electronic structure of the substrate, the absorption step leads to the creation of excited states into the material. The incident photon energy has been transferred to other species, mostly free electrons in upper excited states. Subsequent processes involve relaxation of these excited states and, again, depend on material characteristics and laser parameters. Different processes may take place at the same time into the material: the one with the higher probability to take place (*i.e.* with the shortest characteristic time, τ) will be the dominating one and govern material response [48]. A classification of relaxation processes may be done into thermal and non-thermal.

Thermal processes involve the conversion of excited electron kinetic energy into lattice vibrational energy (phonons) by means of electron-lattice collisions. This phenomenon is also known as thermalization and is characterized by the thermal relaxation time (τ_t). In metals, electron-phonon relaxation times are typically in the order of 10^{-12} to 10^{-11} s [44]. In non-metals, this process is electron-hole recombination via energy transfer to the lattice and its probability is strongly dependent on free carrier density. Typical inter-band electronic excitation may last between 10^{-12} to 10^{-6} s [44]. By means of these mechanisms, thermal equilibrium is reached inside the material: lattice and electrons temperature equalizes.

At this point, it is worthwhile to discuss the role of thermal properties and the differences between good and bad heat conductors. In the former class of materials (all metals and some semiconductors) the thermal diffusivity greatly exceeds the absorption depth: energy will be distributed faster into the bulk material and heat will reach also regions not affected by light exposure. In contrast, thermal insulators with good absorbing properties have thermal diffusion lengths of the same order of the absorption depth.

Conversion of the incident electromagnetic radiation into heating of the material is the most exploited mechanism to process materials, especially for metals. In this case, laser may be thought as a heat-source that can increase the temperature and supply the enthalpy to cause phase change. Then, depending on the temperature reached, melting, vaporization or sublimation of the solid may take place.

If there are other competing processes that take place into the material after photon absorption, the absorbed energy may be redistributed elsewhere, leading to non-thermal relaxation. These other processes can be schematized as:

- photolysis;
- electron ejection and/or photo-ionization;
- electron-hole recombination via non thermal processes.

Photolysis is a process that involves mainly single molecules. The incident photon energy have to exceed its binding energy: when it is absorbed it promotes the molecules to an unstable state that may undergo dissociation. When this happen, the chemical bond is broken and the potential energy stored into the bond is released as kinetic energy of the fragments.

In metals, electron ejection may happen if the incident photon has energy above the working function of the material and it is also known as photoelectric effect. The energy is absorbed by an electron and transformed into its kinetic energy: if this kinetic energy is high enough to overcome the potential barrier of the solid, the electron is ejected from the material.

In non metals, very energetic radiation would be needed to cause this phenomenon in single-step absorption. Therefore it is more prone to happen with multi-photon absorption, associated to high intensities of the incident laser beam. In this case, the electron may gain sufficient kinetic energy and be ejected from the solid, leaving behind an ionized lattice atom. When the density of these photo-ions is sufficient to destabilize the lattice structure itself, a Coulomb explosion may take place: positive ions generate a large and repulsive Coulomb field that causes the ejection of ions, atoms and molecules from the material[47].

In non-metals, the relaxation process of electron-hole recombination may not transfer their energy to the lattice but instead give it to a third carrier inside the material. For semiconductors at high carrier densities (as is the case during high power laser irradiation) Auger recombination is the dominant recombination mode[48]. In this case the recombination energy is given to a third carrier in the valence band, promoting it to the conduction band. Therefore the absorbed energy is not transferred to the lattice but instead is kept inside the free carrier system, that behaves like a plasma inside the solid[48].

All these alternative phenomena have their characteristic time and probability, depending strongly on laser intensity, and may happen only at particular laser conditions, i.e. very short and high power pulses. Furthermore, both thermal and non-thermal processes may take place at the same time.

For the above mentioned reasons, powerful laser irradiation (like that used to machine and modify materials) alters, often drastically, optical properties of many materials. Therefore the interaction between the laser

radiation and the solid becomes a dynamical process and material response changes during irradiation itself. It will not be further possible to describe the material with its fundamental optical properties and time-dependent functions will replace these quantities[48].

1.2.3.4. Laser-induced modifications of materials

As discussed in the previous paragraphs, the laser beam may be thought as an energy source capable of inducing phase change, microstructure modifications and/or thermal stresses inside the material. Again, depending both on material and laser parameters, solid may undergo different phase changes: melting, vaporization, sublimation and plasma formation may occur. Since material response is very sensitive to laser beam characteristics, tuning this device parameters would result in very different material modifications. Fig. 14Fig. 14. Typical timescales and intensity ranges of phenomena and processes of laser-material interaction (reproduced from *[50]*). resumes the phenomena listed above:
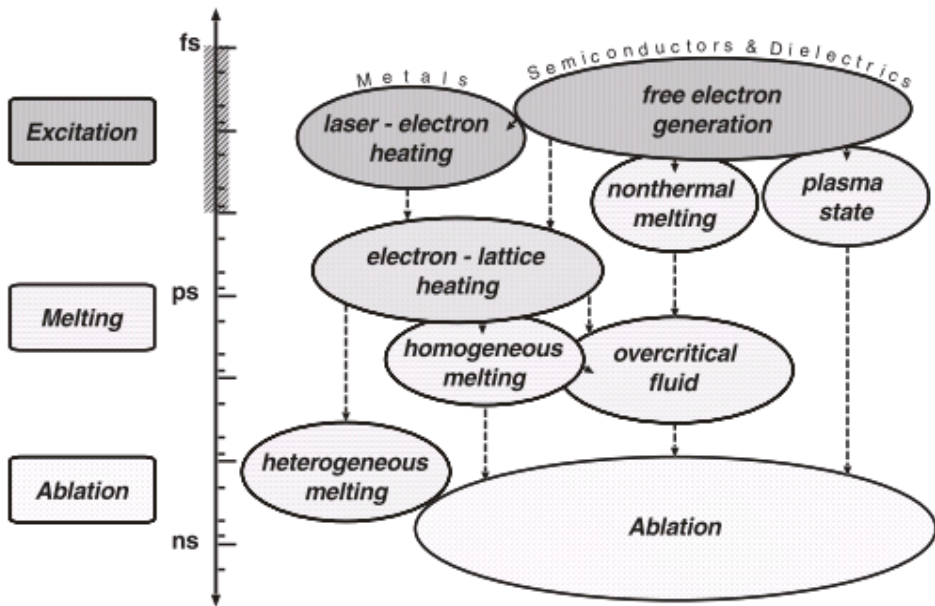
Fig. 14. Typical timescales and intensity ranges of phenomena and processes of laser-material interaction (reproduced from [50]*).*

When a new phase is produced, it interposes between the laser beam and the material itself and further laser absorption is mediated by this new phase. Especially in the case of plasma, since it is composed of charged species

more sensible to electromagnetic radiation, the radiation would be absorbed by this system instead of the solid behind. In extreme cases, the process would turn from laser machining to plasma machining, if the material ends up completely screened by the plasma formed.

1.2.3.5. Laser machining and micropatterning of surfaces

Fabrication of periodic surfaces with micron and submicron feature is a rapidly growing research field with applications in several technological areas. Such structures on the surface of metals, semiconductors, dielectrics and polymers can generate new material properties with very special electrical, mechanical or chemical characteristics. Depending on the specific material parameters and the morphology of the structures, new devices like biosensors, antifraud features, microfluidic devices, templates for biological applications as well as photonic structures can be realized. Furthermore, surface textures can be used to improve tribological properties of special tools, for the reduction of reflection losses or as a decoration element for the refinement of precious goods. Apart from that, photon-based fabrication methods offer several advantages due to their remote and thus contactless operation, their flexibility during materials processing as well as their precise energy deposition [51]. At the micro scale, laser direct writing and lithography techniques are being utilized to pattern and process several materials with features in the range of 1-100 μm.

1.2.4. Direct laser interference patterning

The interference between two or more laser beams can be exploited to produce a distribution of laser intensity on the surface of the material. In this way, based on photo-thermal and/or photo-chemical interactions, the surfaces of the materials could be directly and locally modified at the positions corresponding to interference maxima. This technique is called Direct Laser Interference Patterning (*DLIP*).

To calculate the intensity distribution of an interference pattern it is necessary to add together all (*N*) overlapping laser beams as follows [51]:

$$E = \sum_{j-1}^{N} E_j = \sum_{j-1}^{N} E_{j_0} \, e^{-ik \, \sin \alpha_j (x \cos \beta_j - y \sin \beta_j) + \varphi_j} \qquad (5)$$

where E_j are the amplitudes of the electric field of each j-beam, α_j and β_j which are the angles of the beams with respect to the vertical (polar angle) and the horizontal axis (azimuthal angle)of the interference plan (plane x,y), respectively. φ_j is the initial phase and k the wave number.

Then, the total intensity of the interference pattern can be calculated as:

$$I = \frac{c\,\varepsilon_o}{2}|E| \tag{6}$$

where c is the speed of light and ε_o the permittivity of free space.

Two or more overlapping coherent and linearly polarized laser beams produce an interference pattern with a defined geometry depending on the used wavelength and the angles in between the beams [52]. Depending on the experimental setup (number of beams, beam intensities, incident angle), various intensity distributions can be generated, such as dot-like, line-like and grid-like structures [53].
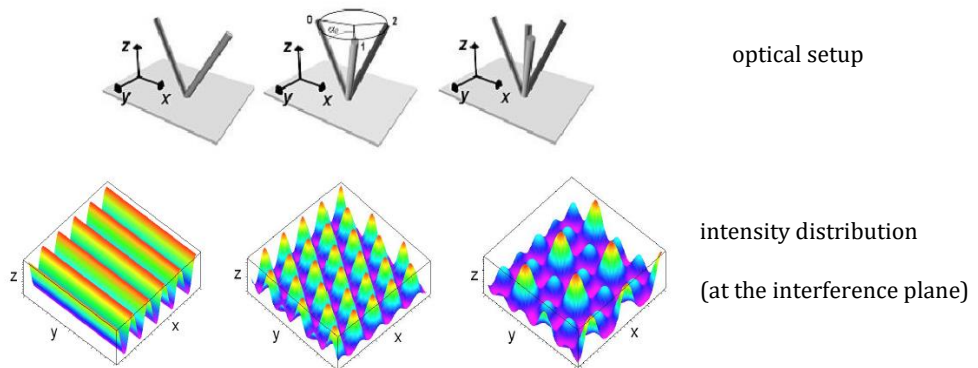
Fig. 15. Intensity patterns obtained with the interference of two (left), three (center) and four (right) beams (adapted from [51]*).*

For two laser beam configuration a one dimensional line-like interference pattern is obtained (as depicted in Fig. 16). Under the aforementioned hypothesis and for two beams with equal intensity, the wave function of the beams (7) and their sum (8) may be written as:

$$E_j = E_o\, e^{i\left(\frac{2\pi r_j}{\lambda} + \omega t\right)} = E_o\, e^{i(kr_j + \varphi_j)} \tag{7}$$

$$E = E_o \left[e^{i(kr_1 + \varphi_1)} + e^{i(k2 + \varphi_2)} \right] \tag{8}$$

Rearranging equations (4) and (5) for the two-beams setup, the intensity distribution reaching the surface of the material may be calculated as follows:

$$I(x) = 2\, I_o \left\{ cos \left[\frac{4\,\pi\,x}{\lambda} \sin\left(\frac{\theta}{2}\right) \right] + 1 \right\} \tag{9}$$

where I_o is the initial intensity of a single beam and λ the wavelength. θ is the incident angle between the two beams. The resulting intensity varies cosinusoidally between $I_{min} = 0$ and $I_{max} = 4I_o$.

The periodicity P (the distance between two maxima, i.e. the distance between two lines) depends on the wavelength of the beam and the optical setup (the angle between the two interfering beams) as follows:

$$P = \frac{\lambda}{2 \sin\theta} \tag{10}$$

This is the simplest achievable geometry but also the easiest setup for technical operation: the line periodicity is not dependent on the phase shift ($\Delta\varphi$) or the misalignment of the sample surface from the interference plane (β_j) [51].

In DLIP nanosecond, picoseconds or femtosecond pulsed lasers are used in order to reach high energy densities at the interference maxima positions during the ultrashort laser pulse interaction with the material. In this way, high peak powers (ranging from MW to GW) can be obtained during irradiation, permitting to locally melt and/or ablate the substrate [54].

A good option for the construction of a DLIP system with ns-pulsed laser is to utilize YAG (Yttrium Aluminum Garnet) lasers with harmonic generators [51]. In this way it is possible to select an appropriated wavelength at which the material has a high absorption, thus tuning the physical phenomena acting during interaction. For example, Nd:YAG lasers (emitting at 1064 nm) cover wavelength ranging from the ultraviolet to the infrared spectrum by frequency doubling (532 nm), tripling (355 nm) and quadrupling (266 nm). Moreover, such system has an impressive coherence length (in the order of some meters) which is necessary to make use of the so-called beam-splitter configuration. The schematic of this setup is shown in Fig. 16:
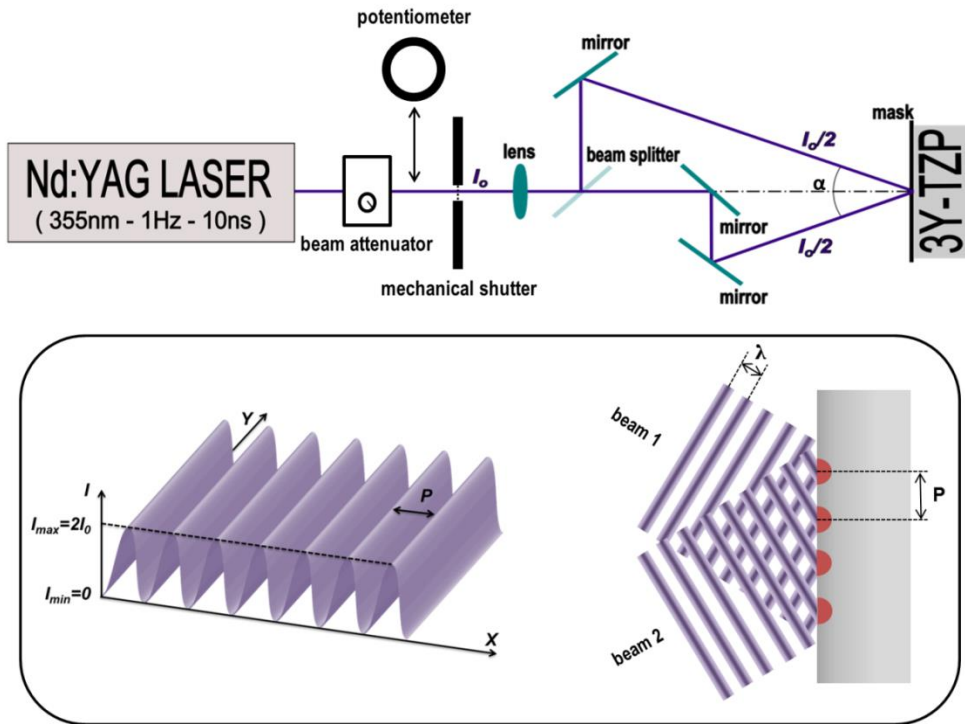
Fig. 16. At the top, optical setup for the beam-splitter configuration. In the inset, laser intensity distribution impinging on the surface (left) thanks to beam interference on the sample (right).

As it can be observed, the primary laser beam is split into two beams to interfere with each other on the sample surface. The optical devices composing the setup are:

- combination of a polarizer and a half-wave plate to adjust the intensity impinging on surface;
- mechanical shutter to control the number of pulses reaching the sample;
- lens to change the diameter of the beam and therefore the power density reaching the material;
- beam splitter to divide the primary beam into two secondary beams with half intensity;
- mirrors to direct the beams to interfere at the sample surface;
- mask to select a squared portion of the laser beam impinging on the surface (in order to make easier the alignment of subsequent adjacent spots for patterning an entire surface).

PHOTO-PHYSICAL MECHANISM
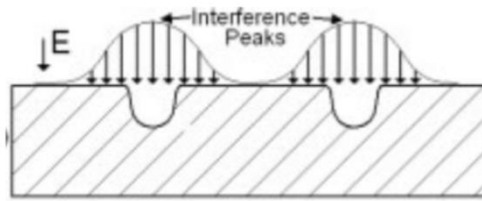
PHOTO-THERMAL MECHANISM
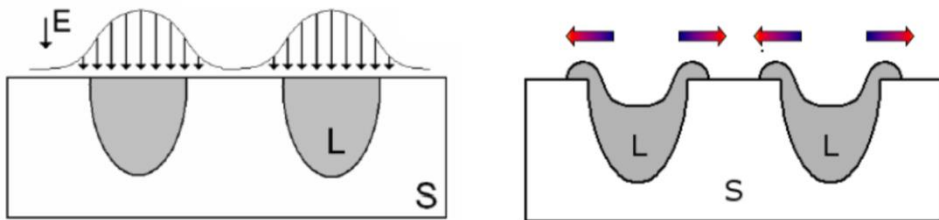
Fig. 17. Sketch of the physical mechanisms allowing the patterning of surfaces with DLIP.

Depending on laser parameters and material characteristics, the physical mechanism activated may result in different topographies. They may be categorized as follows:

- photo-physical: at interference maxima, the material is ablated and/or evaporated and line-trenches are graved. Almost all the ablated material is removed from the sample;
- photo-thermal: at interference maxima, the temperature is increased up to the melting point of the material. If the temperature difference between intensity minima and maxima is high enough, there exist a surface tension gradient and the molten material flows from the hotter zone (lower surface tension) to the cooler zone (higher surface tension). This phenomenon is also called thermo-capillary convection or Marangoni effect [55–57]. If laser parameters are properly tuned, it allows the formation of valleys in correspondence to the molten zone and peaks in correspondence of the resolidified material.

Only one or a combination of the two mechanisms may be activated, depending again on material properties and laser parameters (as for any other laser technique, as introduced previous paragraphs).

In Fig.18Fig. 18. Periodic line (a-c), cross (d) and hierarchical patterns (e) fabricated on stainless steel and titanium. Different optical setup and laser parameters result in very different topographies, also with the simplest two beam configuration (reproduced from *[51]*). are given some examples of achievable patterns on metals:
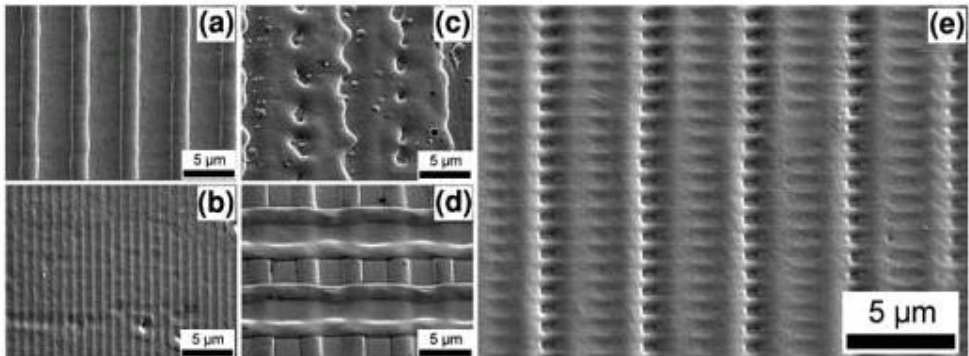
Fig. 18. Periodic line (a-c), cross (d) and hierarchical patterns (e) fabricated on stainless steel and titanium. Different optical setup and laser parameters result in very different topographies, also with the simplest two beam configuration (reproduced from [51]*).*

1.3. Surface patterning of dental grade zirconia (3Y-TZP)

1.3.1. Surface modification and patterning of 3Y-TZP

A lot of research has been focused on surface modification and functionalization of zirconia dental restorations [42] to improve the biological response or the mechanical adhesion to other materials (for instance, enamels or dental cements and resins). Surface roughening has been demonstrated to promote osseointegration and it can be achieved by sandblasting [58], grinding [59] or acid etching [60]. Surface patterning has been proven to be capable of cell guidance [61] and to increase the adhesion to dental cement [62] and porcelain [63]. Unfortunately, the fabrication of defined micropatterns smaller than 100 μm is still considered challenging [43] due to the hardness and brittleness of ceramics. Defined patterns can be produced by mechanical micromachining, stamp transfer molding and laser-

based techniques [64]. The last is considered promising and a valid alternative to classical mechanical methods because it is faster, more accurate in pattern reproduction [65] and it is relatively easy to implement. Furthermore, being a non-contact technology it is of special interest in the biomedical field since it may produce lower surface contamination [66].
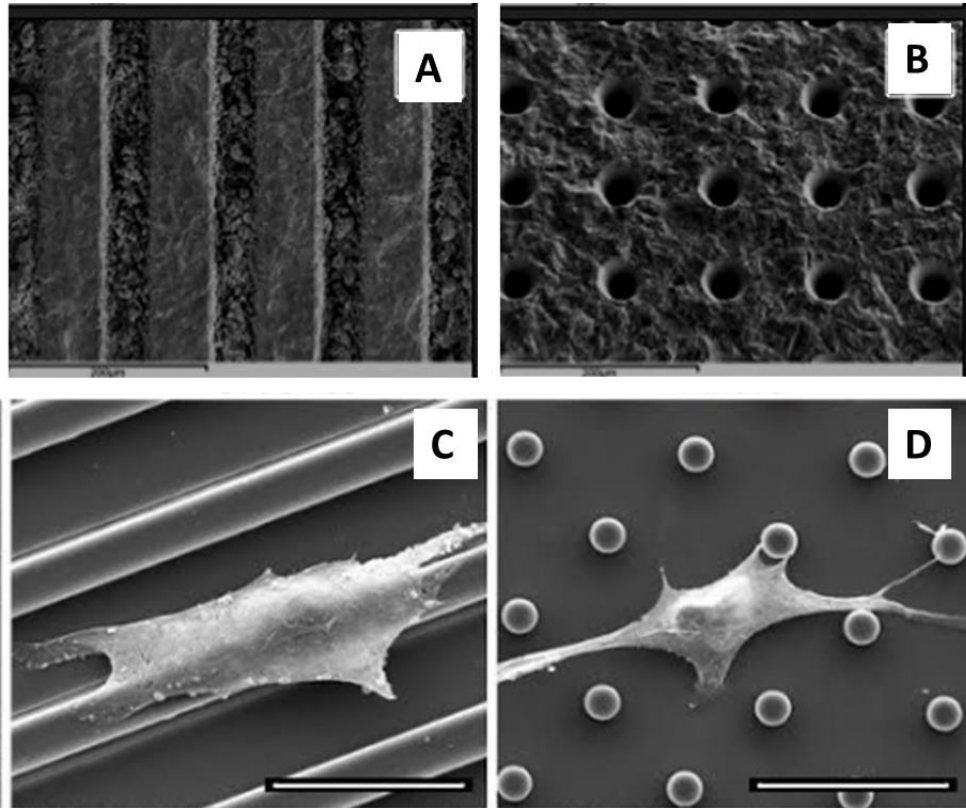
Fig. 19. Examples of zirconia patterned surfaces for biomedical applications: (A, B) fs-laser patterning with grooves and pits (reproduced from [67]) and silica grooves and pillars ([61])

Surface treatments on 3Y-TZP generally introduce collateral damage and microstructural modifications in the remaining material: sandblasting [58], grinding [59] and acid etching [68] have already been proven to affect its microstructure and therefore mechanical properties and long-term stability. In fact, the transformation toughening behavior depends on the stress-induced transformability of the retained tetragonal structure to monoclinic phase. Therefore, 3Y-TZP is very sensitive to any alteration in the density, grain size, presence of residual stresses, stabilizer content and distribution, even locally [7]. Laser treatments can produce severe surface damage and microstructural or compositional modifications mainly due to

the thermal loads caused by laser-material interaction [69]. It is therefore of paramount importance to evaluate the impact of a laser-based surface treatment on the microstructure of such material.

1.3.2. Laser machining and patterning of 3Y-TZP

Short-pulsed laser treatments are commonly used to machine metallic and ceramic materials and modify topography, chemical and physical properties of surfaces [43]. Monochromatic, coherent and high brightness electromagnetic radiation is exploited as an energy source to locally remove or modify the material. Depending both on laser parameters (wavelength, pulse duration, pulse number and fluence) and material properties (optical and thermal), different physical mechanisms are activated [44]. Incoming energy is absorbed by the electronic system and then may be converted to thermal energy or other form of kinetic energy of charged species. In semiconductors and insulators in the short pulse regime, the energy absorbed by the electronic system mostly ends up in the ionization of lattice atoms. When a critical density of charged species is reached, Coulomb repulsion leads to a "Coulomb explosion" [49], i.e. material ablation. This is the most well-recognized mechanism for laser material ablation, also for Y-TZP [70],[71],[72]. However, some energy may also be transferred from electrons to lattice phonons, i.e. heat production, leading to microstructural changes and phase transformation (typically melting, vaporization and plasma formation). On the other hand, the extremely high absorbed energy density reached inside the irradiated volume may increase density and pressure to levels high enough to produce unexpected phase and microstructural modifications [10]. YSZ are heat-sensitive materials since even slight variation in its composition, phase and microstructure or the formation of microcracks and residual stresses are capable of strongly affect its mechanical properties and long term stability [2,26]. Therefore, it is desirable to reduce thermal load on the untreated volume, that is to reduce the heat affected zone (i.e. the thermal diffusion length) [73].

In the literature, several papers report on different kind of laser treatments on dental zirconia for different applications: from machining of implant components [62,74–77] to surface patterning of the implant to increase bone adhesion [22],[23]. Different lasers sources (that may be sorted according to the emitted wavelength into the two big sub-categories of infrared [20],[23–27] and ultraviolet [20],[21],[24],[25]) working at different regimes (continuous wave [21],[25] and pulsed [62,67,70–72,74–76,78,80–

82]) have been tested and reported. Within the latter regime, pulses from microsecond to femtosecond duration have been exploited. Lasers are characterized by many different parameters influencing the density of energy reaching the material and the resulting interaction with the material (the absorption depth strongly depends on the wavelength and the pulse duration, for example). Therefore, it is not straightforward to compare different treatments and how they affect the material. However, some general and common conclusions may be drawn and many groups agree on some general observations about the effect of laser treatment on dental YSZ:

- cracking on the surface of the material [18–20],[24–26] and in the bulk [76];
- increment in surface roughness[12],[23–26];
- pore formation[22],[25].
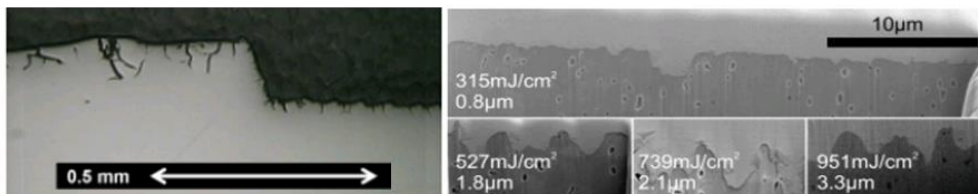
Fig. 20. On the left, the cross-section (optical microscopy) of dental-grade zirconia surface machined with a ps (left) and ns (right) laser source (reproduced from [76]): severe cracking is observed with a strong dependence on pulse duration. On the right, the cross section (FIB and SEM) of 5Y-TZP treated with ns-DLIP: roughening of the surface and pore formation (reproduced from [70]).

Even if laser treatments some times are presented as collateral damage-free methods [67], there is evidence of material modification and possible introduction of defects (cracks and pores). Since mechanical properties and LTD resistance of 3Y-TZP strongly depend on microstructural features, care should be taken on the effect of laser treatment on the microstructure and stability of such materials.

There are few papers [20],[22],[25] reporting on the impact of laser modifications on mechanical properties of 3Y-TZP. In their study, C. Daniel and colleagues [78] applied direct interference patterning with an ultraviolet nanosecond pulsed laser source while J. Parry and his group [76] used a direct-writing technique to grave lines and trenches, with both an infrared and ultraviolet nanosecond and picoseconds pulsed laser sources. C. Daniel et al. [78] reported an increment in three-point bending strength for laser treated samples and determines a set of laser parameters that allow up to a 50% increment. J. Parry [76] reported a decrease in four-point bending

strength, both with nanosecond and picoseconds treatments, correlated to the introduction of micrometric size cracks. The two groups disagree about the positive or detrimental effect of the laser treatment on mechanical properties but, since the resulting surface modifications slightly differ, the two papers should be compared carefully. These observations emphasize the importance of a more complete characterization of the modifications induced in the material, especially in the volume just below the surface. Furthermore, the influence on LTD has not been investigated until now, even if it is a key topic for dental applications [10].

To conclude, taking into account the studies reported until now, it may be concluded that laser treatment is a suitable method to machine and modify dental zirconia material. However, it is far from being free of collateral damage in the remaining volume and a characterization of the modifications induced is desirable, with a correlation to mechanical properties at short and long term. All the latter aspects have been taken into consideration in the literature, but results are scattered and sometime contradictory. A more systematic and parametric work is advisable.

2. Main objectives and structure of the thesis

There is an increasing interest in the functionalization of the surface of dental zirconia with the aim of improving the performances of dental implants, posts and prosthesis. This ranges from enhancing biomaterial adhesion to different synthetic substrates, to medical implant integration, tissue engineering applications and spatial control of cells on materials. These goals may be achieved through the control and tuning of topographical features in the size range of biological species (i.e. from micrometric to nanometric scale). Laser-based techniques are a valid tool to introduce geometric patterns on the surface of biomaterials because they allow high precision and repeatability at micrometric scale. Furthermore, surface patterning of ceramic material at the micrometric scale is still considered challenging because of the intrinsic brittleness of this family of materials and laser-based techniques are regarded as a promising tool since they involve no contact with the substrate. Direct Laser Interference Patterning (DLIP) is especially effective and fast in the production of periodical geometries at the micrometric scale, exploiting beam interference on the treated surface.

In this thesis DLIP has been employed to pattern the surface of 3Y-TZP. Laser treatment on zirconia ceramics may be challenging because of the high sensitivity of this family of materials to any change in their microstructure. Their mechanical properties, especially fracture toughness, and resistance to low temperature degradation strongly depends on the meta-stabilization of the tetragonal phase at room temperature. This in turn depends on local chemical composition, density, grains size, porosity and residual stresses state of the material. Laser interaction with matter in the nanosecond regime produces mainly thermal effect. Due to the low thermal coefficient of zirconia, that may result in the local alteration of microstructure, the formation of a heat affected zone and in thermal shock on the surface. Therefore, it is of paramount importance to understand the type and magnitude of microstructural changes and collateral damage produced after laser-material interaction in 3Y-TZP to ensure the short and long term stability of the treated material.

Therefore, the main objectives of this thesis are:

- to optimize DLIP parameters to produce periodical topographies on dental grade zirconia;
- to assess the microstructural changes produced during laser treatment, especially in terms of damage, phases of the material and change in grain size and composition;
- to investigate any change in the resistance to low temperature degradation of this material after laser treatment, as well as to explore methods to enhance LTD resistance;
- to measure the change in mechanical properties of the laser treated materials, with special interest in mechanical reliability of these materials.

Special attention will be paid on correlating laser-induced microstructural changes to the mechanical properties and LTD resistance of 3Y-TZP, in order to guarantee material reliability after laser treatment.

In order to achieve these objectives, the thesis has been structured as follows.

In *chapter 3*, an extensive summary of the academic work will detail the connections between papers and how they could be regarded as a whole project.

In *chapter 4*, general conclusions and proposals for future work are established.

In *paper I,* the achievable topographies and the geometrical characteristics of the pattern will be assessed as a function of laser parameters (fluence and number of pulses). Optimal combination of parameters is proposed. Results are published in "E. Roitero, F. Lasserre, M. Anglada, F. Mücklich, E. Jiménez-Piqué, A parametric study of laser interference surface patterning of dental zirconia: effects of laser parameters on topography and surface quality, *Dental Materials 33 (2016), e28–e38"* and this publication is included as chapter.

In *paper II,* a detailed characterization of the microstructure resulting after laser treatment will be performed: both changes produced on the surface and inside the bulk will be considered. This aims not only to describe the eventual collateral damage produced in the treated material, but also to understand the physical phenomena taking place during laser material interaction and the pattern formation mechanism. Results are published in "E. Roitero, F. Lasserre, J.J. Roa, M. Anglada, F. Mücklich, E. Jiménez-Piqué, Nanosecond-laser patterning of 3Y-TZP: damage and microstructural

changes, *Journal of the European Ceramic Society **37** (2017), 4876–4887"* and this publication is included as chapter.

In *paper III*, the kinetics of LTD will be characterized to test if DLIP is a suitable technique to grant the long-term reliability of patterned 3Y-TZP. An annealing treatment after laser patterning is proposed as an effective mean to increase LTD resistance of the treated material. The results are published in "E. Roitero, M. Ochoa, M. Anglada, F. Mücklich, E. Jiménez-Piqué, Low temperature degradation of laser patterned 3Y-TZP: enhancement of resistance after thermal treatment, *Journal of the European Ceramic Society (2017)"* (article in press, accepted on 21/10/2017) and this publication is included as chapter.

In *paper IV (annex A)*, the mechanical properties of laser patterned dental zirconia will be tested to guarantee the short term integrity of the treated material. The minor decrease in properties is explained in terms of laser-induced damage. The results are being submitted for publication.

3. Summary of the main results

In this chapter a summary of the most relevant results of this work is presented. Taken together, the academic works contribute to understand how nanosecond laser interference patterning modifies the topography and microstructure of 3Y-TZP and how these changes influence the integrity and reliability of the material after the laser treatment. Special care has been paid on the hydrothermal degradation resistance of this family of material after the laser patterning, due to their susceptibility to microstructural changes caused by surface treatments.
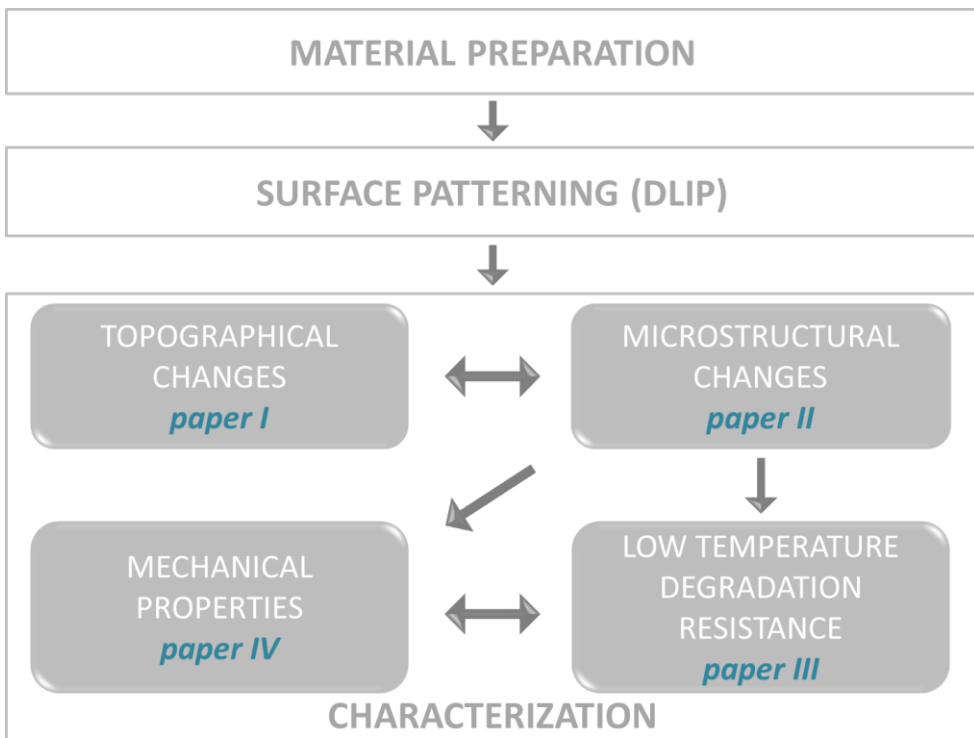
Fig. 21. Scheme of the structure of the thesis and how the papers included can be considered as a whole work.

3.1. Paper I

A parametric study of laser interference surface patterning of dental zirconia: effects of laser parameters on topography and surface quality.

E. Roitero, F. Lasserre, M. Anglada, F. Mücklich, E. Jiménez-Piqué.

The aim of this work is to generate micrometric linear patterns with different topography on dental grade zirconia by means of laser interference and to assess the quality of the produced surface, both in term of the geometry produced and of the surface damage induced in the material.
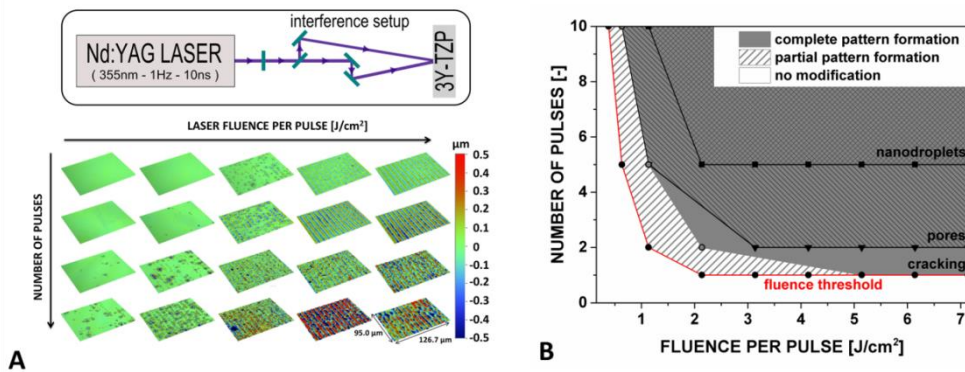
Fig. 22. In A, WLI images of the effect of laser fluence and number of pulses on the topography of the surfaces of 3-YTZP. In B, a damage map compiles the defects introduced by laser treatment as a function of fluence and number of pulses.

Results show that line-patterning of zirconia surfaces can be achieved with periodicities comprised within 5 and 15 μm. Tuning laser parameters allows varying independently pattern depth, overall roughness and surface finish. Increasing both fluence and number of pulses allows producing deeper patterns (maximum achievable depth of 1 μm). However, increasing the number of pulses has a detrimental effect on the quality of the produced lines. Surface damage (intergranular cracking, open porosity and nano-droplets formation) can be generated, depending on laser parameters.

Best conditions in terms of quality of the produced pattern and minimum material damage is obtained for low number of pulses with high laser fluence. Zirconia materials with controlled topography can be produced

with this method, which are expected to enhance biological response and mechanical performance of dental components.

3.2. Paper II

Nanosecond-laser patterning of 3Y-TZP: damage and microstructural changes.

E. Roitero, F. Lasserre, J.J. Roa, M. Anglada, F. Mücklich, E. Jiménez-Piqué

The aim of this study is to characterize in detail the microstructural changes and collateral damage induced by direct laser patterning on the surface of dental-grade zirconia (3Y-TZP) employing an interference setup with the 532 and 355 nm harmonics of a Nd:YAG laser (pulse duration of 10 ns).
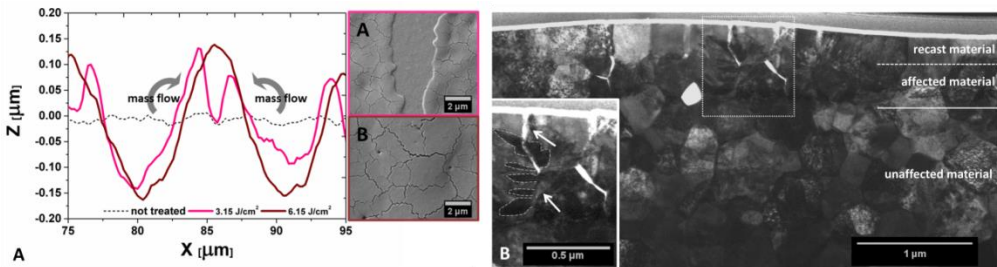
Fig. 23. In A, a scheme of the pattern formation mechanism involving melting and material flow due to capillary forces. In B, BF-STEM image of the region of material below a topography peak. Twinning and microcracking are evident in the inset.

Laser-material interaction mainly results in thermal effects for both wavelengths studied. Upon laser irradiation the material locally melts producing pattern and establishing a steep thermal gradient on the surface. This generates a ~ 1 μm thick heat affected zone where microcracking, directional recrystallization, phase transformation (from tetragonal to monoclinic, $t{\rightarrow}m$) and texturization (ferroelastic domain switching) take place. In addition, surface coloration results from the activation of F-centers

as a consequence of high energy radiation exposure. No chemical segregation or diffusion was detected.
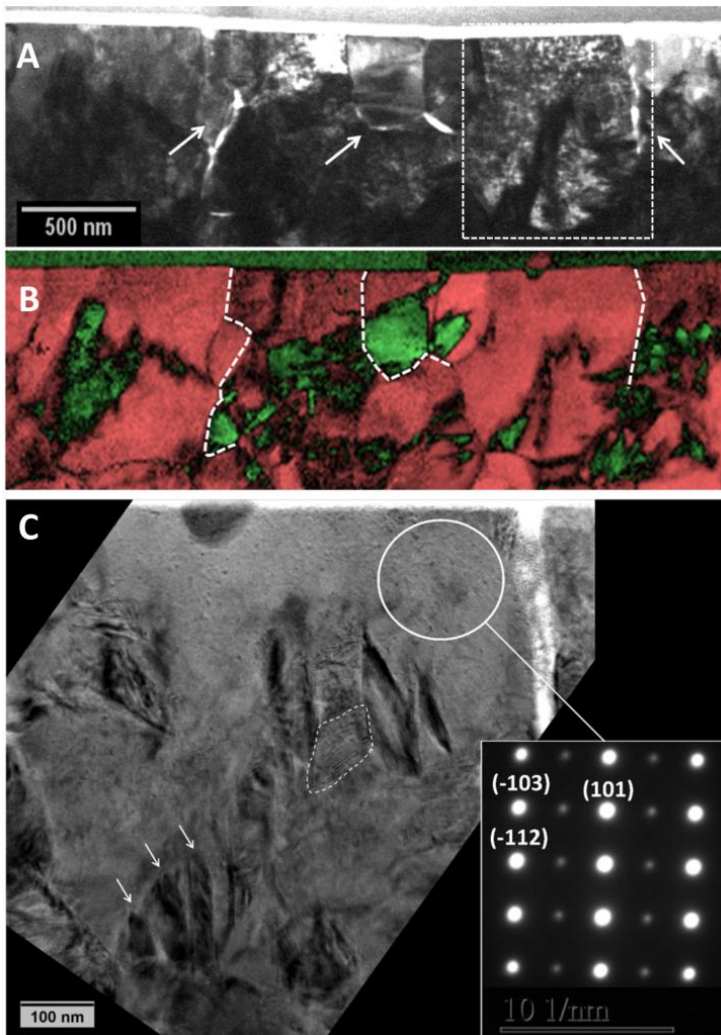
Fig. 24. Phases distribution in the surface affected layer of treated material.

The existence of cracks and phase transformation raise the question of reliability of the material. Although the short cracks will not compromise mechanical strength, the long-term effects are worth being studied. In addition, low temperature degradation resistance may be modified by the presence of monoclinic phase, microcracks and grain texturization.

This paper can be read on page 77.

.

3.3. Paper III

Low temperature degradation of laser patterned 3Y-TZP: enhancement of resistance after thermal treatment.

E. Roitero, M. Ochoa, M. Anglada, F. Mücklich, E. Jiménez-Piqué.

The aim of this study is to characterize the resistance to LTD)of the surface of dental-grade zirconia (3Y-TZP) patterned with a Nd:YAG laser (532 nm harmonic and pulse duration of 10 ns) employing an interference setup.
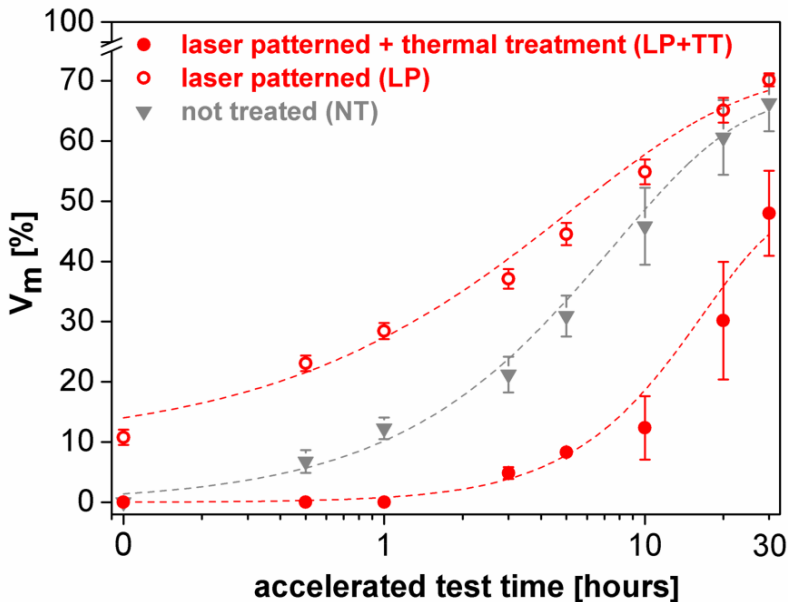
Fig. 25. Kinetics of LTD in vapor at 131°C.

Laser patterning decreases the resistance to LTD of 3Y-TZP because of the presence of monoclinic phase and residual stresses, induced by the thermal shock during laser-material interaction. A thermal treatment (1 hour at 1200°C) anneals the affected microstructure and strongly increase the resistance to LTD of laser patterned 3Y-TZP. Transformation is delayed thanks to monoclinic phase reversion, texture in the tetragonal phase and the existence of a net of shallow microcracks on the surface, accommodating autocatalytic transformation. Therefore, a thermal treatment is strongly

recommended after laser patterning of 3Y-TZP to ensure the long-term stability of the treated surface.

This paper can be read on page 91.

3.4. Paper IV

Mechanical reliability of laser patterned 3Y-TZP.

E. Roitero, M. Anglada, F. Mücklich, E. Jiménez-Piqué.

To be submitted

The aim of this work is to characterize the fracture strength and the integrity of the surface of dental-grade zirconia (3Y-TZP) modified with direct laser patterning, employing an interference setup with the 532 nm harmonics of a Nd:YAG laser (pulse duration of 10 ns).
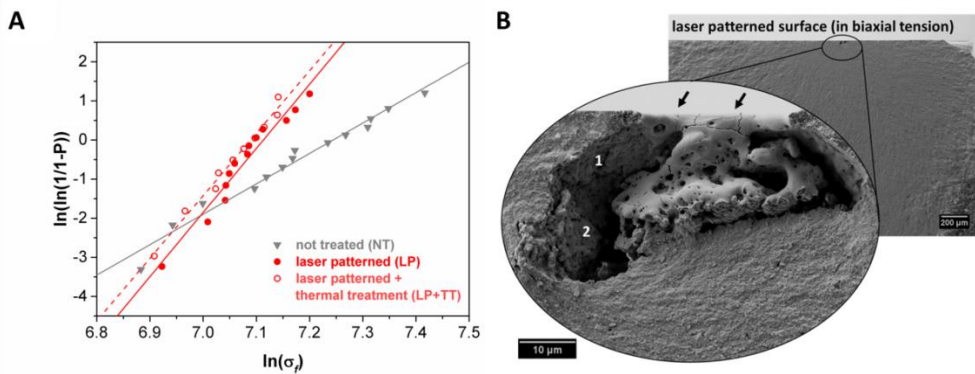
Fig. 26. In A, the Weibull distribution of laser patterned 3Y-TZP compared to not treated material. In B, a FESEM image of a surface critical defect: laser beam interacts with a pre-existing defect causing an enlargement of the flaw.

Laser patterning with DLIP induces a minor decrease in mechanical properties and surface integrity of 3Y-TZP. The biaxial strength (B3B) and the hardness and Young modulus of the treated surfaces decrease as a consequence of the damage induced by laser patterning. Laser-affected layer could not be at the origin of fractures alone since its thickness is only 1 μm, well below the critical defect size. Surprisingly, laser interaction with pre-

existing defects close to the surface result in an enlargement of such surface defects, thanks to focalization of laser radiation and subsequent material melting and damage. Those enlarged critical defects may be at the origin of the decrease in Weibull characteristic strength and the increase in Weibull modulus. On the other side, the affected layer caused by laser exposure is at the origin of the decrease in hardness and Young modulus of the surface. Microcracking in particular should be the main responsible of it, even if it seems not to strongly compromise surface integrity upon scratching.

A thermal treatment after laser patterning does not alter further surface integrity and mechanical properties of laser patterned 3Y-TZP.

This paper can be read on page 101.

4. Main conclusions and future work

4.1. Main conclusions

From the results and discussions included in this thesis some general conclusions can be drawn, in the attempt to answer to the objectives proposed:

1. It is possible to introduce a periodical micrometric-sized pattern on the surface of 3Y-TZP with DLIP. By tuning laser parameters (fluence and number of pulses) the roughness and the aspect ratio of the pattern can be varied independently. Optimal laser parameters combination to produce a well-defined topography (although with minor aspect ratio) is high fluence with low pulse number.

2. DLIP in the nanosecond regime produces mainly thermal effects on 3Y-TZP. The pattern forms on the surface thanks to material melting and molten flow due to capillary forces.

3. Laser treatment allows the desired alteration of surface topography, however, it also induces some collateral damage and microstructural modifications. Columnar grains, intergranular microcracking, $t \rightarrow m$ phase transformation, t-phase texturization and residual stresses are all concentrated in an affected layer of ≈ 1 µm below the treated surface. All these alterations are a consequence of the steep thermal gradients arising during laser treatment

4. Laser treatment induces a minor decrease in the mechanical properties of 3Y-TZP. The affected layer is not the cause of fracture, being the damage too shallow to be a critical defect. However, the interaction of the laser beam with pre-existing porosities causes the enlargement of such critical defects, reducing the strength of the treated material.

5. Laser treatment reduces the LTD resistance of 3Y-TZP, mainly because of the presence of m-phase.

6. A thermal treatment at 1200°C for 1h enhances the LTD resistance of laser patterned 3Y-TZP. The annealing is able to revert the $t \rightarrow m$ phase transformation, maintaining the texture in the t-phase and the surface topography intact. This results in a retardation of transformation, increasing the resistance to LTD even further that of not treated material.

7. The exposure to highly energetic electromagnetic radiation induces the activation of *F*-centers, i.e. change in color of the treated surfaces. A thermal treatment at 1200°C of 1h restores the withe color of 3Y-TZP.

Therefore, the answer to the main question "Is DLIP a suitable method to pattern the surface of 3Y-TZP?" would be affirmative, but with due caution. Even if the collateral damage induced by thermal effects of the laser treatment is confined in a very thin layer of material, not being a concern for its short term integrity, it may be a serious concern on the long term. It is therefore important to stress the necessity to perform a simple thermal treatment (at 1200°C for 1 h) after laser patterning, to ensure LTD resistance. Furthermore, an optimal surface finish, ideally free of defects, is a key factor to reduce the ability of laser to enlarge critical defects and so reduce the mechanical strength.

4.2. Future work

Based on the results presented in this thesis, an outlook of possible research trends is proposed in this paragraph.

1. Investigation about the origin and morphology of the texture in t-phase induced by the laser treatment. The presence of texture in the portion of material close to the treated surface has been observed with XRD and is compatible with ferroelastic domain switching. The fact that this texturization is maintained even after the annealing treatment is at the origin of the increment in LTD resistance and, therefore, deserves a detailed study. The identification of the ferroelastic domains, which may be tetragonal domains with different orientations inside a single 200-300 nm grain, is not a trivial topic due to their nanometric size. This topic should be addressed to an HR-TEM study.

2. Investigation about the amount and distribution of residual stresses caused by laser treatment. The presence of residual stresses as a consequence of the steep thermal gradients arising during laser treatment and phase transformation has been observed indirectly as peaks widening in XRD measurements. However, their quantification is not straightforward with traditional laboratory diffractometers, since stresses are highly concentrated and probably distributed inhomogeneously inside the volume assessed with X-Rays. Therefore,

a employing a synchrotron source would allow reaching higher resolution and determine their magnitude and arrangement.

3. Test of different laser sources with shorter pulses (i.e. in the ps and fs regimes) to pattern 3Y-TZP. As observed in this study, the physical mechanisms activated by ns-pulsed laser in zirconia are mainly thermal, resulting in material melting and evaporation. This, in turn, induces the formation of a heat affected zone in the remaining material, which is at the origin of the loss of LTD resistance. Employing a different laser source may solve the problem of the collateral damage. These ultrashort pulsed lasers have been already employed for patterning with direct writing techniques, giving interesting results, but have not yet been tested with an interference setup.

4. Investigation about the biological response to the patterned surfaces. Once the treated material has been proven to be safe for application, it would be interesting to test the efficacy of the pattern on biological species behavior. The geometry and size of the micrometric periodic pattern and the roughness on a shorter length-scale may be varied with DLIP on 3Y-TZP and the influence of these different characteristics on cells behavior could be tested. Change of topography produced with DLIP could also be coupled with other surface functionalization techniques, aiming at improving further surface properties for biomedical applications.

References

[1]   R. Hannink, P.M. Kelly, B.C.. Muddle, Transformation Toughening in Zirconia-Containing Ceramics, J. Am. Ceram. Soc. 83 (2000) 461–487. http://onlinelibrary.wiley.com/doi/10.1111/j.1151-2916.2000.tb01221.x/abstract (accessed December 16, 2013).

[2]   V. Lughi, V. Sergo, Low temperature degradation -aging- of zirconia: A critical review of the relevant aspects in dentistry., Dent. Mater. 26 (2010) 807–20. doi:10.1016/j.dental.2010.04.006.

[3]   J. Chevalier, What future for zirconia as a biomaterial?, Biomaterials. 27 (2006) 535–43. doi:10.1016/j.biomaterials.2005.07.034.

[4]   R.C. GARVIE, R.H. HANNINK, R.T. PASCOE, Ceramic steel?, Nature. 258 (1975) 703–704. http://dx.doi.org/10.1038/258703a0.

[5]   J. Chevalier, B. Cales, J.M. Drouin, Low-Temperature Aging of Y-TZP Ceramics, J. Am. Ceram. Soc. 54 (1999) 2150–2154.

[6]   Implants for surgery — Ceramic materials based on yttria-stabilized tetragonal zirconia (Y-TZP) - EN ISO 13356:2013, (2013).

[7]   J. Chevalier, L. Gremillard, A. V. Virkar, D.R. Clarke, The Tetragonal-Monoclinic Transformation in Zirconia: Lessons Learned and Future Trends, J. Am. Ceram. Soc. 92 (2009) 1901–1920. doi:10.1111/j.1551-2916.2009.03278.x.

[8]   J. Kelly, I. Denry, Stabilized zirconia as a structural ceramic: an overview., Dent. Mater. 24 (2008) 289–98. doi:10.1016/j.dental.2007.05.005.

[9]   A.G. Evans, Perspective on the Development of High-Toughness Ceramics, J. Am. Ceram. Soc. 73 (1990) 187–206.

[10]   J. Chevalier, L. Gremillard, S. Deville, Low-Temperature Degradation of Zirconia and Implications for Biomedical Implants, Annu. Rev. Mater. Res. 37 (2007) 1–32. doi:10.1146/annurev.matsci.37.052506.084250.

[11]   M. Hisbergues, S. Vendeville, P. Vendeville, Zirconia: Established facts and perspectives for a biomaterial in dental implantology., J. Biomed. Mater. Res. B. Appl. Biomater. 88 (2009) 519–29. doi:10.1002/jbm.b.31147.

[12]   X. Guo, Low temperature degradation mechanism of tetragonal zirconia ceramics in water: role of oxygen vacancies, Solid State Ionics. 112 (1998) 113–116. doi:10.1016/S0167-2738(98)00212-4.

[13]   X. Guo, T. Schober, Water Incorporation in Tetragonal Zirconia, J. Am. Ceram. Soc. 87 (2004) 746–748. doi:10.1111/j.1551-2916.2004.00746.x.

[14]   T. Duong, A.M. Limarga, D.R. Clarke, Diffusion of water species in yttria-stabilized zirconia, J. Am. Ceram. Soc. 92 (2009) 2731–2737. doi:10.1111/j.1551-2916.2009.03271.x.

[15]   L. Gremillard, J. Chevalier, T. Epicier, S. Deville, G. Fantozzi, Modeling the aging kinetics of zirconia ceramics, J. Eur. Ceram. Soc. 24 (2004) 3483–3489. doi:10.1016/j.jeurceramsoc.2003.11.025.

[16]   J.A. Muñoz-Tabares, E. Jiménez-Piqué, M. Anglada, Subsurface evaluation of hydrothermal degradation of zirconia, Acta Mater. 59 (2011) 473–484. doi:10.1016/j.actamat.2010.09.047.

[17]   F. Zhang, M. Inokoshi, K. Vanmeensel, B. Van Meerbeek, I. Naert, J. Vleugels, Lifetime estimation of zirconia ceramics by linear ageing kinetics, Acta Mater. 92 (2015) 290–298. doi:10.1016/j.actamat.2015.04.001.

[18]   J. Cotič, P. Jevnikar, A. Kocjan, Ageing kinetics and strength of airborne-particle abraded 3Y-TZP ceramics, Dent. Mater. 3 (2017) 1–10. doi:10.1016/j.dental.2017.04.014.

[19]   J.W. Christian, Ch01: General Introduction, in: Theory Transform. Met. Alloy., 2002: pp. 1–22. doi:http://dx.doi.org/10.1016/B978-008044019-4/50005-2.

[20]   M. Cattani-Lorente, S.S. Scherrer, S. Durual, C. Sanon, T. Douillard, L. Gremillard, J. Chevalier, A. Wiskott, Effect of different surface treatments on the hydrothermal degradation of a 3Y-TZP ceramic for dental implants, Dent. Mater. 30 (2014) 1136–1146. doi:10.1016/j.dental.2014.07.004.

[21]   F. Zhang, K. Vanmeensel, M. Batuk, J. Hadermann, M. Inokoshi, B. Van Meerbeek, I. Naert, J. Vleugels, Highly-translucent, strong and aging-resistant 3Y-TZP ceramics for dental restoration by grain boundary segregation, Acta Biomater. 16 (2015) 215–222. doi:10.1016/j.actbio.2015.01.037.

[22]   R. Garvie, P. Nicholson, Phase analysis in zirconia systems, J. Am. Ceram. …. (1972) 303–305. doi:10.1111/j.1151-2916.1972.tb11290.x.

[23]   H. Toraya, M. Yoshimura, S. Somiya, Calibration Curve for Quantitative Analysis of the Monoclinic-Tetragonal ZrO2 System by X-Ray Diffraction., Commun. Am. Ceram. Soc. 67 (1984) C119–C121. doi:10.1111/j.1151-2916.1984.tb19715.x.

[24]   J. Chevalier, L. Gremillard, Ceramics for medical applications: A picture for the next 20 years, J. Eur. Ceram. Soc. 29 (2009) 1245–1255. doi:10.1016/j.jeurceramsoc.2008.08.025.

[25]   C. Piconi, G. Maccauro, Zirconia as a ceramic biomaterial., Biomaterials. 20 (1999) 1–25. http://www.ncbi.nlm.nih.gov/pubmed/9916767.

[26]   I. Denry, J. Kelly, State of the art of zirconia for dental applications., Dent. Mater. 24 (2008) 299–307. doi:10.1016/j.dental.2007.05.007.

[27]   J.M. Powers, R.L. Sakaguchi, Craig's Restorative Dental Materials, 12th ed., Elsevier, 2006.

[28]   B. Kasemo, Biological surface science, Curr. Opin. Solid State Mater. Sci. 3 (1998). http://www.sciencedirect.com/science/article/pii/S003960280101809X (accessed April 29, 2014).

[29]   A. Gristina, Biomaterial-centered infection: microbial adhesion versus tissue integration. 1987., Science (80-.). 237 (1987). http://www.ncbi.nlm.nih.gov/pubmed/15552128.

[30]   H.J. Busscher, M. Rinastiti, W. Siswomihardjo, H.C. van der Mei, Biofilm formation on dental restorative and implant materials., J. Dent. Res. 89 (2010) 657–65. doi:10.1177/0022034510368644.

[31]   C. Bollen, P. Lambrechts, M. Quirynen, Comparison of surface roughness of oral hard materials to the threshold surface roughness for bacterial plaque retention: a review of the literature, Dent. Mater. (1997) 258–269. http://www.sciencedirect.com/science/article/pii/S0109564197800383 (accessed November 24, 2014).

[32]   L. Rimondini, L. Cerroni, A. Carrassi, P. Torricelli, Bacterial Colonization of Zirconia Ceramic Surfaces: An in Vitro and in Vivo Study,

Int. J. Oral Maxillofac. Implant. 17 (2002) 793–798.
http://www.scopus.com/inward/record.url?eid=2-s2.0-0036835660&partnerID=tZOtx3y1.

[33] C. Do Nascimento, M.S. Pita, V. Pedrazzi, R.F. de Albuquerque Junior, R.F. Ribeiro, In vivo evaluation of Candida spp. adhesion on titanium or zirconia abutment surfaces., Arch. Oral Biol. 58 (2013) 853–61. doi:10.1016/j.archoralbio.2013.01.014.

[34] C. Do Nascimento, M.S. Pita, F.H.N.C. Fernandes, V. Pedrazzi, R.F. de Albuquerque Junior, R.F. Ribeiro, Bacterial adhesion on the titanium and zirconia abutment surfaces., Clin. Oral Implants Res. 25 (2014) 337–43. doi:10.1111/clr.12093.

[35] C. Do Nascimento, C. da Rocha Aguiar, M.S. Pita, V. Pedrazzi, R.F. de Albuquerque, R.F. Ribeiro, Oral biofilm formation on the titanium and zirconia substrates., Microsc. Res. Tech. 76 (2013) 126–32. doi:10.1002/jemt.22143.

[36] M. Quirynen, C.M. Bollen, The influence of surface roughness and surface-free energy on supra- and subgingival plaque formation in man. A review of the literature., J. Clin. Periodontol. 22 (1995) 1–14. http://www.scopus.com/inward/record.url?eid=2-s2.0-0029193280&partnerID=tZOtx3y1.

[37] W. Teughels, N. Van Assche, I. Sliepen, M. Quirynen, Effect of material characteristics and/or surface topography on biofilm development., Clin. Oral Implants Res. 17 Suppl 2 (2006) 68–81. doi:10.1111/j.1600-0501.2006.01353.x.

[38] Z. Wang, Y. Shen, M. Haapasalo, Dental materials with antibiofilm properties., Dent. Mater. 30 (2014) e1–e16. doi:10.1016/j.dental.2013.12.001.

[39] L. Karygianni, A. Jähnig, S. Schienle, F. Bernsmann, E. Adolfsson, R. Kohal, J. Chevalier, E. Hellwig, A. Al-Ahmad, Initial Bacterial Adhesion on Different Yttria-Stabilized Tetragonal Zirconia Implant Surfaces in Vitro, Materials (Basel). 6 (2013) 5659–5674. doi:10.3390/ma6125659.

[40] G.R. de Oliveira, L. Pozzer, L. Cavalieri-Pereira, P.H. de Moraes, S. Olate, J.R. de Albergaría Barbosa, Bacterial adhesion and colonization differences between zirconia and titanium implant abutments:

an in vivo human study., J. Periodontal Implant Sci. 42 (2012) 217–23. doi:10.5051/jpis.2012.42.6.217.

[41]   A. Wennerberg, T. Albrektsson, On implant surfaces: a review of current knowledge and opinions., Int. J. Oral Maxillofac. Implants. 25 (2009) 63–74. http://www.ncbi.nlm.nih.gov/pubmed/20209188.

[42]   L. Treccani, T. Yvonne Klein, F. Meder, K. Pardun, K. Rezwan, Functionalized ceramics for biomedical, biotechnological and environmental applications., Acta Biomater. 9 (2013) 7115–50. doi:10.1016/j.actbio.2013.03.036.

[43]   M.G. Holthaus, L. Treccani, K. Rezwan, Comparison of micropatterning methods for ceramic surfaces, J. Eur. Ceram. Soc. 31 (2011) 2809–2817. doi:10.1016/j.jeurceramsoc.2011.07.020.

[44]   D.W. Bäuerle, Laser processing and chemistry, 4th ed., Springer, 2011.

[45]   W.M. Steen, Laser Material Processing, 3rd ed., Springer, 2003.

[46]   J.C. Ion, Laser processing of engineering materials, 1st ed., Elsevier, 2005.

[47]   J. Brannon, Excimer laser ablation and etching, 1st ed., American Vacuum Society, 1993.

[48]   M. von Allmen, A. Blatter, Laser-beam interaction with materials, 2nd ed., Springer, 1995.

[49]   E.G. Gamaly, a. V. Rode, Physics of ultra-short laser interaction with matter: From phonon excitation to ultimate transformations, Prog. Quantum Electron. 37 (2013) 215–323. doi:10.1016/j.pquantelec.2013.05.001.

[50]   B. Rethfeld, K. Sokolowski-Tinten, D. von der Linde, S.I. Anisimov, Timescales in the response of materials to femtosecond laser excitation, Appl. Phys. A. 79 (2004) 767–769. doi:10.1007/s00339-004-2805-9.

[51]   A.F.. Lasagni, F.A.. Lasagni, Fabrication and characterization in the micro-nano range, 2011.

[52]   C. Daniel, F. Mücklich, Z. Liu, Periodical micro-nano-structuring of metallic surfaces by interfering laser beams, Appl. Surf. Sci. 208-209 (2003) 317–321. doi:10.1016/S0169-4332(02)01381-8.

[53]   M. Hans, F. Müller, S. Grandthyll, S. Hüfner, F. Mücklich, Anisotropic wetting of copper alloys induced by one-step laser micro-patterning, Appl. Surf. Sci. 263 (2012) 416–422.

[54]   J.R.. Lawrence, C.. Dowding, J.B.. Griffiths, eds., Laser surface engineering: processes & applications, Elsevier, 2014.

[55]   T.D. Bennett, D.J. Krajnovich, C.P. Grigoropoulos, P. Baumgart, a C. Tam, Marangoni mechanism in pulsed laser texturing of magnetic disk substrates, J. Heat Transf. Asme. 119 (1997) 589–596. doi:10.1115/1.2824146.

[56]   S. Berg, Marangoni-driven spreading along liquid-liquid interfaces, Phys. Fluids. 21 (2009). doi:10.1063/1.3086039.

[57]   A. Karbalaei, R. Kumar, H. Cho, Thermocapillarity in Microfluidics—A Review, Micromachines. 7 (2016) 13. doi:10.3390/mi7010013.

[58]   R.K. Chintapalli, F.G. Marro, E. Jimenez-Piqué, M. Anglada, Phase transformation and subsurface damage in 3Y-TZP after sandblasting, Dent. Mater. 29 (2013) 566–572. doi:10.1016/j.dental.2013.03.005.

[59]   J.A. Muñoz-Tabares, E. Jimenez-Piqué, J. Reyes-Gasga, M. Anglada, Microstructural changes in ground 3Y-TZP and their effect on mechanical properties, Acta Mater. 59 (2011) 6670–6683. doi:10.1016/j.actamat.2011.07.024.

[60]   Q. Flamant, F. García Marro, J.J. Roa Rovira, M. Anglada, Hydrofluoric acid etching of dental zirconia. Part 1: etching mechanism and surface characterization, J. Eur. Ceram. Soc. 36 (2015) 121–134. doi:10.1016/j.jeurceramsoc.2015.09.021.

[61]   M.S. Laranjeira, Â. Carvalho, A. Pelaez-Vargas, D. Hansford, M.P. Ferraz, S. Coimbra, E. Costa, A. Santos-Silva, M.H. Fernandes, F.J. Monteiro, Modulation of human dermal microvascular endothelial cell and human gingival fibroblast behavior by micropatterned silica coating surfaces for zirconia dental implant applications, Sci. Technol. Adv. Mater. 15 (2014) 025001. doi:10.1088/1468-6996/15/2/025001.

[62]   N. Bärsch, S. Barcikowski, K. Baier, Ultrafast-Laser-Processed Zirconia and its Adhesion to Dental Cement, J. Laser Micro/Nanoengineering. 3 (2008) 78–83. doi:10.2961/jlmn.2008.02.0004.

[63]   D. Liu, J.P. Matinlinna, J.K.H. Tsoi, E.H.N. Pow, T. Miyazaki, Y. Shibata, C.W. Kan, A new modified laser pretreatment for porcelain zirconia bonding, Dent. Mater. 29 (2013) 559–565. doi:10.1016/j.dental.2013.03.002.

[64]   M.G. Holthaus, S. Twardy, J. Stolle, O. Riemer, L. Treccani, E. Brinksmeier, K. Rezwan, Micromachining of ceramic surfaces: Hydroxyapatite and zirconia, J. Mater. Process. Technol. 212 (2012) 614–624. doi:10.1016/j.jmatprotec.2011.06.007.

[65]   A.N. Samant, N.B. Dahotre, Laser machining of structural ceramics—A review, J. Eur. Ceram. Soc. 29 (2009) 969–993. doi:10.1016/j.jeurceramsoc.2008.11.010.

[66]   A. Kurella, N.B. Dahotre, Review paper: surface modification for bioimplants: the role of laser surface engineering., J. Biomater. Appl. 20 (2005) 5–50. doi:10.1177/0885328205052974.

[67]   R. a Delgado-Ruiz, J.L. Calvo-Guirado, P. Moreno, J. Guardia, G. Gomez-Moreno, J.E. Mate-Sanchez, P. Ramirez-Fernández, F. Chiva, Femtosecond laser microstructuring of zirconia dental implants., J. Biomed. Mater. Res. B. Appl. Biomater. 96 (2011) 91–100. doi:10.1002/jbm.b.31743.

[68]   Q. Flamant, M. Anglada, Hydrofluoric acid etching of dental zirconia. Part 2: effect on flexural strength and ageing behavior, J. Eur. Ceram. Soc. 36 (2015) 135–145. doi:10.1016/j.jeurceramsoc.2015.09.022.

[69]   B.S. Yilbas, Y.A.-D. Ahmad, A.-A. Nasser, M.A.-Q. Hussain, Materials Forming, Machining and Tribology - Laser Pulse Heating of Surfaces and Thermal Stress Analysis, 2014.

[70]   C. Daniel, B.L. Armstrong, J.Y. Howe, N. Dahotre, Controlled Evolution of Morphology and Microstructure in Laser Interference-Structured Zirconia, J. Am. Ceram. Soc. 91 (2008) 2138–2142. doi:10.1111/j.1551-2916.2008.02449.x.

[71]   N. Bärsch, K. Werelius, S. Barcikowski, F. Liebana, U. Stute, A. Ostendorf, Femtosecond laser microstructuring of hot-isostatically pressed zirconia ceramic, J. Laser Appl. 19 (2007) 107–115.

http://www.scopus.com/inward/record.url?eid=2-s2.0-34249013742&partnerID=40&md5=4591dcd6d32bfe0d3fd7aa0f41aaa621.

[72]   S. Heiroth, J. Koch, T. Lippert, a. Wokaun, D. Günther, F. Garrelie, M. Guillermin, Laser ablation characteristics of yttria-doped zirconia in the nanosecond and femtosecond regimes, J. Appl. Phys. 107 (2010) 014908. doi:10.1063/1.3275868.

[73]   J. Cheng, C. Liu, S. Shang, D. Liu, W. Perrie, G. Dearden, K. Watkins, A review of ultrafast laser materials micromachining, Opt. Laser Technol. 46 (2013) 88–102. doi:10.1016/j.optlastec.2012.06.037.

[74]   J. Parry, R. Ahmed, F. Dear, J. Shephard, M. Schmidt, L. Li, D. Hand, A Fiber-Laser Process for Cutting Thick Yttria-Stabilized Zirconia: Application and Modeling, Int. J. Appl. Ceram. Technol. 8 (2011) 1277–1288. doi:10.1111/j.1744-7402.2010.02559.x.

[75]   J. Parry, J.D. Shephard, F. Dear, N. Jones, N. Weston, D. Hand, Nanosecond-Laser Postprocessing of Millisecond- Laser-Machined Zirconia (Y-TZP) Surfaces, Int. J. Appl. Ceram. Technol. 5 (2008) 249–257. doi:10.1111/j.1744-7402.2008.02222.x.

[76]   J. Parry, J.D. Shephard, D. Hand, C. Moorhouse, N. Jones, N. Weston, Laser Micromachining of Zirconia (Y-TZP) Ceramics in the Picosecond Regime and the Impact on Material Strength, Int. J. Appl. Ceram. Technol. 8 (2011) 163–171. doi:10.1111/j.1744-7402.2009.02420.x.

[77]   T. Kizaki, T. Ogasahara, N. Sugita, M. Mitsuishi, Ultraviolet-laser-assisted precision cutting of yttria-stabilized tetragonal zirconia polycrystal, J. Mater. Process. Technol. 214 (2014) 267–275. doi:10.1016/j.jmatprotec.2013.09.015.

[78]   C. Daniel, J. Drummond, R.A. Giordano, Improving Flexural Strength of Dental Restorative Ceramics Using Laser Interference Direct Structuring, J. Am. Ceram. Soc. 91 (2008) 3455–3457. doi:10.1111/j.1551-2916.2008.02642.x.

[79]   P.P. Shukla, J. Lawrence, Role of laser beam radiance in different ceramic processing: A two wavelengths comparison, Opt. Laser Technol. 54 (2013) 380–388. doi:10.1016/j.optlastec.2013.06.011.

[80]   S. Stübinger, F. Homann, C. Etter, M. Miskiewicz, M. Wieland, R. Sader, Effect of Er : YAG, CO2 and diode laser irradiation on

surface properties of zirconia endosseous dental implants, LASERS Surg. Med. 40 (2008) 223–228. doi:10.1002/lsm.20614.

[81]   F. Dear, J.D. Shephard, X. Wang, J.D.C. Jones, D. Hand, Pulsed laser micromachining of yttria-stabilized zirconia dental ceramic for manufacturing, Int. J. Appl. Ceram. Technol. 5 (2008) 188–197. doi:10.1111/j.1744-7402.2008.02203.x.

[82]   J. Ihlemann, A. Scholl, H. Schmidt, B. Wolff-Rottke, Nanosecond and femtosecond excimer-laser ablation of oxide ceramics, Appl. Phys. A. 60 (1995). http://link.springer.com/article/10.1007/BF01538343 (accessed March 19, 2014).

[83]   R.-J. Kohal, W. Att, M. Bächle, F. Butz, Ceramic abutments and ceramic oral implants . An update, Periodontol. 2000. 47 (2008) 224–243.

[84]   Y. Ito, Surface micropatterning to regulate cell functions., Biomaterials. 20 (1999) 2333–42. http://www.ncbi.nlm.nih.gov/pubmed/10614939.

[85]   E. Roitero, F. Lasserre, M. Anglada, F. Mücklich, E. Jiménez-Piqué, A parametric study of laser interference surface patterning of dental zirconia: Effects of laser parameters on topography and surface quality, Dent. Mater. (2016) 10–14. doi:10.1016/j.dental.2016.09.040.

[86]   W.D. Kingery, H.K. Bowen, D.R. Uhlmann, Introduction to ceramics, 2nd ed., Wiley, 1976.

[87]   E. Roitero, F. Lasserre, J.J. Roa, M. Anglada, F. Mücklich, E. Jiménez-Piqué, Nanosecond-laser patterning of 3Y-TZP: Damage and microstructural changes, J. Eur. Ceram. Soc. 37 (2017) 4876–4887. doi:10.1016/j.jeurceramsoc.2017.05.052.

[88]   R. Danzer, A general strength distribution function for brittle materials, J. Eur. Ceram. Soc. 10 (1992) 461–472. doi:10.1016/0955-2219(92)90021-5.

[89]   P.P. Shukla, J. Lawrence, Characterization and compositional study of a ZrO2 engineering ceramic irradiated with a fibre laser beam, Opt. Laser Technol. 43 (2011) 1292–1300. doi:10.1016/j.optlastec.2011.03.026.

[90]   B.S. Yilbas, Laser treatment of zirconia surface for improved surface hydrophobicity, J. Alloys Compd. 625 (2015) 208–215. doi:10.1016/j.jallcom.2014.11.069.

[91]   E. Roitero, M. Ochoa, M. Anglada, F. Mücklich, E. Jiménez-Piqué, Low temperature degradation of laser patterned 3Y-TZP: Enhancement of resistance after thermal treatment, J. Eur. Ceram. Soc. in press (2017) 0–1. doi:10.1016/j.jeurceramsoc.2017.10.044.

[92]   M. Hans, C. Gachot, F. Müller, F. Mücklich, Direct laser interference structuring as a tool to gradually tune the wetting response of titanium and polyimide surfaces, Adv. Eng. Mater. 11 (2009) 795–800. doi:10.1002/adem.200900115.

[93]   R. Danzer, W. Harrer, P. Supancic, T. Lube, Z. Wang, A. B??rger, The ball on three balls test-Strength and failure analysis of different materials, J. Eur. Ceram. Soc. 27 (2007) 1481–1485. doi:10.1016/j.jeurceramsoc.2006.05.034.

[94]   A. Börger, P. Supancic, R. Danzer, The ball on three balls test for strength testing of brittle discs: stress distribution in the disc, J. Eur. Ceram. Soc. 22 (2002) 1425–1436. doi:10.1016/S0955-2219(01)00458-7.

[95]   W. Weibull, A statistical distribution function of wide applicability, J. Appl. Mech. 18 (1951) 293–297. doi:citeulike-article-id:8491543.

[96]   D. Munz, T. Fett, Ceramics : mechanical properties, failure behaviour, materials selection, Springer, 1999. doi:10.1007/978-3-642-33848-9.

[97]   W.C. Oliver, G.M. Pharr, Measurement of hardness and elastic modulus by instrumented indentation: Advances in understanding and refinements to methodology, J. Mater. Res. 19 (2004) 3–20. doi:10.1557/jmr.2004.19.1.3.

[98]   Y. Gaillard, M. Anglada, E. Jiménez-Piqué, Nanoindentation of yttria-doped zirconia: Effect of crystallographic structure on deformation mechanisms, J. Mater. Res. 24 (2009) 719–727. doi:10.1557/jmr.2009.0091.

[99]   Y. Gaillard, E. Jiménez-Piqué, F. Soldera, F. Mücklich, M. Anglada, Quantification of hydrothermal degradation in zirconia by

nanoindentation, Acta Mater. 56 (2008) 4206–4216. doi:10.1016/j.actamat.2008.04.050.

[100] A.C. Fischer-Cripps, A review of analysis methods for sub-micron indentation testing ⚬, Vacuum. 58 (2000) 569–585.

[101] R. Danzer, On the relationship between ceramic strength and the requirements for mechanical design, J. Eur. Ceram. Soc. 34 (2014) 3435–3460. doi:10.1016/j.jeurceramsoc.2014.04.026.

[102] M. Turon-Vinas, M. Anglada, Fracture toughness of zirconia from a shallow notch produced by ultra-short pulsed laser ablation, J. Eur. Ceram. Soc. 34 (2014) 3865–3870. doi:10.1016/j.jeurceramsoc.2014.05.009.

[103] K. Noguchi, M. Fujita, T. Masaki, M. Mizushina, Tensile Strength of Yttria-Stabilized Tetragonal Zirconia Polycrystals, J. Am. Ceram. Soc. 72 (1989) 1305–1307. doi:10.1111/j.1151-2916.1989.tb09736.x.

[104] S.G. Demos, M. Staggs, M.R. Kozlowski, Investigation of processes leading to damage growth in optical materials for large-aperture lasers., Appl. Opt. 41 (2002) 3628–3633. doi:10.1364/AO.41.003628.

[105] H. Bercegol, P. Grua, D. Hebert, J.P. Morreeuw, Progress in the understanding of fracture related laser damage of fused silica - art. no. 672003, Laser-Induced Damage Opt. Mater. 2007. 6720 (2008) 72003. doi:10.1117/12.752830.

[106] L. Ceseracciu, M. Anglada, E. Jiménez-Piqué, Hertzian cone crack propagation on polycrystalline materials: Role of R-curve and residual stresses, Acta Mater. 56 (2008) 265–273. doi:10.1016/j.actamat.2007.09.030.

Paper I

A parametric study of laser interference surface patterning of dental zirconia:
effects of laser parameters on topography and surface quality

P1

P2

P3

P4

P5

P6

P7

P8

P8

9

P10

P11

Paper II

Nanosecond-laser patterning of 3Y-TZP: damage and microstructural changes

P1

2

3

4

5

6

7

8

9

10

11

12

Paper III

Low temperature degradation of laser patterned 3Y-TZP:enhancement of resistance after thermal treatment

1

2

3

4

5

6

7

8

Paper IV

Mechanical reliability of laser patterned 3Y-TZP

Mechanical reliability of laser patterned 3Y-TZP

E. Roitero, M. Anglada, F. Mücklich, E. Jiménez-Piqué
Manuscript to be submitted

1. Introduction

Tetragonal Zirconia Polycrystal stabilized with 3 mol. % Y_2O_3 (3Y-TZP) is being increasingly used in dentistry, both for prosthesis and implants, due to an excellent combination of biocompatibility, mechanical performance and aesthetics [6]. Nowadays, there is also an increasing interest towards the implementation of ceramic oral implants as an alternative to the golden standard of titanium [83] due to their higher resistance to bio-corrosion and superior esthetic properties.

A lot of research has been focused on surface modification and functionalization [42] of these restorations to improve the biological response or the mechanical adhesion to other materials (enamels or dental cements and resins). Each application may require a different kind of topography, in terms of geometry, regularity and scale-size (generally, the desired features are in the micro- and nano-scale [84]). Unfortunately, the fabrication of defined micropatterns smaller than 100 µm is still considered challenging [43] due to the hardness and brittleness of ceramics. Defined patterns can be produced by mechanical micromachining, stamp transfer molding and laser-based techniques [64]. The last is considered promising and a valid alternative to classical mechanical methods because it is faster, more accurate in pattern reproduction [65] and it is relatively easy to implement. Furthermore, being a non-contact technology it is of special interest in the biomedical field since it may produce lower surface contamination [66].

Direct Laser Interference Patterning (DLIP) offers a fast and accurate alternative to introduce controlled topography at the micrometric and sub-micrometric scale [65]. In this technique a periodical intensity distribution is produced by beam interference on the surface of the material to be treated. Depending on the number of interfering laser beams and the optical setup, different geometries can be produced (lines or dots). Laser pulse melts locally the substrate and capillary forces generated thanks to temperature difference on the surface cause material flow and pattern formation [85]. Due to the

shortness of the laser pulse and the low thermal conductivity of 3Y-TZP [86], a very steep thermal gradient is established on the treated surface, which results in thermal shock. This produces recrystallization in form of columnar grains growing perpendicularly to the surface and intergranular microcracking, down to 1 μm depth. The high thermal load induces also $t \rightarrow m$ phase transformation, texturization of t-phase and residual stresses and strains. Furthermore, the highly energetic laser irradiation activates color centers (mostly electrons trapped in charged oxygen vacancies). The total and local chemical composition of the surface is not altered by the laser exposure. All these modifications are homogeneously distributed along the topography and affect the first micrometer of material below the treated surface. Further details about type and distribution of collateral damages after laser treatment can be found in [87].

Understanding the effect of such microstructural changes induced by DLIP on the mechanical properties of 3Y-TZP is of paramount importance in order to ensure material reliability. Since in ceramic materials fracture is governed by critical defects [88], it is necessary to understand how the laser treatment could affect defect population and distribution, especially on the surface. At date, few studies [78,89,90] about the mechanical properties of laser patterned zirconia have been reported and mainly involved hardness measurements alone [89,90]. Only C. Daniel *et al.* [78] have tested uniaxial flexural strength of dental grade zirconia patterned with DLIP: they reported a notable increment in flexural strength attributed to the nanometric size grains and compressive residual stresses caused by laser treatment. However, it is not possible to generalize such observations since laser treatments encompass a wide variety of effects of laser interaction with matter resulting in very different microstructural changes [87]. In this study we tested the effect of the surface treatment on the biaxial flexural strength and performed fractographic analysis in an attempt to understand which the critical defects are. Surface hardness and Young modulus were tested with nanonindentation in order to evaluate the integrity of the laser affected layer. We tried to correlate the laser induced damages and modifications with variations in mechanical performances. The long term reliability of the laser patterned material has already been discussed in a previous work about the low temperature degradation (LTD) of laser patterned surface of 3Y-TZP [91].

2. Materials and methods

2.1. Material processing

Commercially available powder of Tetragonal Polycrystalline Zirconia stabilized with 3% molar Y_2O_3 (TZ-3YSB-E, Tosoh, Tokyo, Japan) was cold-isostatic pressed at 200 MPa and then sintered at 1450°C for two hours (3°C/min heating rate). The rods were cut into discs of approximately 9 mm diameter and 2mm thickness. The surface of the samples was ground and polished with diamond suspensions of $30 - 6 - 3$ µm particle size with a final step of colloidal silica. The measured final density was 6.03 ± 0.02 g/cm³ (99.67% of theoretical density) with a grain size of 0.31 ± 0.08 µm (intercept distance). The obtained material has biomedical grade, according to ISO 13356:2013 [6]. These samples were then split into two groups: the first group did not undergo any further modification while the other discs were laser patterned with DLIP. The samples that did not undergo any further treatment were labelled Not Treated (NT) and served as reference material. The discs that were laser-treated were labelled Laser Patterned (LP) and were further divided into two groups: one group (LP) did not undergo any further treatment after patterning while the other discs (LP+TT) were annealed after the laser treatment. The annealing treatment was performed in an air furnace at 1200°C during 1 hour, with the purpose of eliminating residual stresses and revert the monoclinic phase to tetragonal (further details about the effect of the thermal treatment on LP samples can be found in [91]).

2.2. Laser patterning

A Q-switched Nd:YAG laser (Spectra Physics Quanta-Ray PRO210) with a fundamental wavelength of 1064nm was employed in the DLIP setup. The output wavelength of 532 nm obtained by second harmonic generation was used for patterning of zirconia discs surface. The repetition rate and the pulse duration of the laser were 10 Hz and 10 ns, respectively. All samples were treated with one single pulse and with a fluence of 4 J/cm². An optical setup with two interfering beams allows producing a striped pattern consisting of alternating valleys and peaks with a peak-to-peak distance (i.e. periodicity) of 10 µm. The two-beam interference results in a plane sinusoidal intensity distribution $I(x,y)$ on the surface of the sample, as schematized in [85]. It can be described by:

$$I(x,y) = I_o \left[cos \left(\frac{4\pi x}{\lambda} \sin \alpha \right) + 1 \right]$$

(1)

where I_o is the intensity of the laser beam before splitting, λ is the laser wavelength and α is the half angle between the interfering beams. Further details about the technique and the setup employed can be found in [52] and [92].

2.3. Flexural test and fractography

The biaxial strength of NT, LP and LP + TT discs was tested with the ball on three balls (B3B) method [93]. Fracture load was measured on discs subjected to biaxial flexure with a testing fixture with cobalt-cemented tungsten carbide balls of 5.9 mm diameter and a loading rate of 200 N/s, using a servo-hydraulic testing machine (8511, Instron). Then, the biaxial strength was calculated according to the numerical approximation proposed by Börger *et al.* in [94]:

$$\sigma_f = f \left(\frac{t}{R}, \frac{R_a}{R}, v \right) \cdot \frac{F}{t^2}$$

(2)

where F is the fracture load, t is the sample thickness and f is a dimensionless parameters depending on the geometry of the disc (the radius of the disc R, the support radius $R_a = 3.4$ mm and the Poisson's ratio $v \approx 0.3$ for 3Y-TZP, see [94] for further details).

A statistical analysis of the results was performed applying the conventional Weibull theory [95,96]. The distribution function is defined as:

$$P(\sigma_f) = 1 - e^{-\left(\frac{\sigma_f}{\sigma_0} \right)^m}$$

(3)

where P is the cumulative probability of failure, σ_f is the biaxial strength, σ_o is the Weibull characteristic strength, and m is the Weibull modulus.

For the graphical evaluation of m and σ_o (liner regression) the measured strength data were ranked in increasing order and numbered from 1 to N. Then, the single strength values $\sigma_{f\,i}$ were related to the failure probability P_i according to the following relation:

$$P_i = \frac{1 - 0.5}{N}$$

(4)

where i is the ranking number and N is the total number of measurements.

Observation of the fracture surfaces and identification of fracture origin was performed with Scanning Electron Microscopy (SEM) (Neon 40, Carl Zeiss).

2.4. Nanoindentation and scratch test

The integrity and mechanical properties of treated surfaces were assessed with nanoindentation. Tests were performed using a MTS Nanoindenter XP with a continuous stiffness measurement module and with a Berkovich diamond tip calibrated against fused silica standard. Results were analyzed with the Oliver and Pharr method [97].

Scratch test were performed with a CMS Revetest using a Rockwell C diamond tip, with increasing load from 0 N to 60 N with a scratch length of 2 mm.

3. RESULTS

3.1. Strength analysis

The mean biaxial flexural strength results are shown in Table 1. Both LP and LP+TT samples show a slight decrease in strength compared to NT samples. There is no significant difference between the strength of laser patterned samples before (LP) and after (LP+TT) the thermal treatment.

	σ_f [MPa]	σ_o [MPa]	m
Not Treated (NT)	1347 ± 64	1400	7.8 ± 0.6
Laser Patterned (LP)	1190 ± 81	1228	16.4 ± 1.1
Laser Patterned + Thermal Treatment (LP+TT)	1161 ± 112	1199	16.0 ± 0.7

Table 1. Mean biaxial strength (σ_f), Weibull characteristic strength (σ_o) and Weibull modulus (m) for NT, LP and LP+TT samples.

Weibull analysis (Fig.1, Table 1) confirmed the decrease of strength associated to laser patterning. The distribution of the results of LP and LP+TT samples is not only shifted towards lower strength values but it is also less

scattered, if compared to NT samples. This is evidenced in the increase of the Weibull modulus (Table 1). Again, the thermal treatment after laser patterning has no substantial influence.
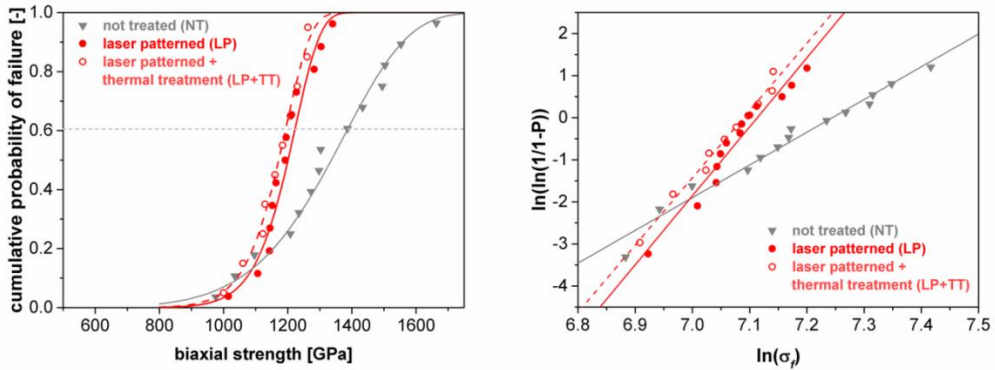

Fig. 1: Weibull distributions of not treated (NT, grey triangles) and laser patterned before (LP, hollow red circles) and after thermal treatment (LP+TT, red circles). (A) Linear scale and (B) logarithmic scale graph.

Because of the limited number of samples, interpretations regarding the Weibull distribution have to be subjected to caution. It seems, however, that laser patterning plays some role on the critical defect size and distribution.

3.2. Fractography

In all tested samples, fracture initiated at the center of the disc on the surface undergoing biaxial tension, as expected since this is the volume of the disc experiencing the highest tensile stresses [94]. Identification of fracture origins in LP and LP+TT samples was possible because a mirror zone was present on all examined discs (Fig. 2A, B). However, it was not always possible to identify univocally the critical defect (Fig. 3B).
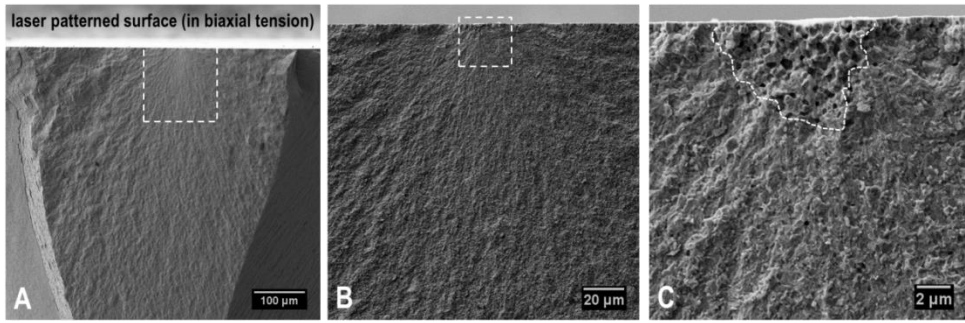
Fig. 2: FESEM images of the fracture surface of a LP sample (σ_f = 1143 MPa). (A) A mirror zone can be identified as the origin of fracture on the laser treated surface undergoing biaxial tension in the central area of the disc (maximum stress). In (B), the magnification of the mirror zone region allows to identify the fracture origin as a defect close to the laser treated surface. In (C), the critical defect responsible of fracture can be identified as porous

The identification of critical defects was possible both in LP and LP+TT samples: processing defects like porosity (Fig. 3A, C, D) or low density regions (Fig. 2 C) were found to be at the origin of fracture for both group of samples. Also in this case no substantial difference was observed between LP and LP+TT samples.
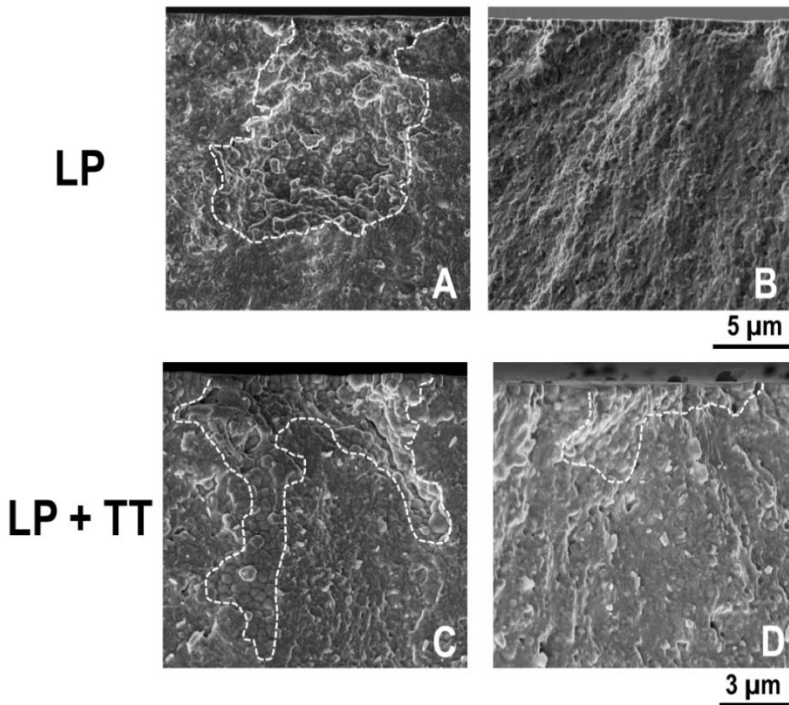

Fig. 3: FESEM images of critical defects at the origin of fracture of LP (A, B) and LP+TT samples (C, D). Biaxial strength of each samples is 1015 MPa (A), 1304 MPa (B), 1128 MPa (C) and 1263 MPa (D), respectively. In (B) the critical defect could not be identified.

The fracture in the mirror region close to the laser treated surface is transgranular, both in LP and LP+TT samples (see Fig. 4A). With a closer look (Fig. 4B), it is possible to distinguish a thin layer of intergranular fracture ($\approx$ 1 µm thick) corresponding to the first layer of grains below the treated surface.
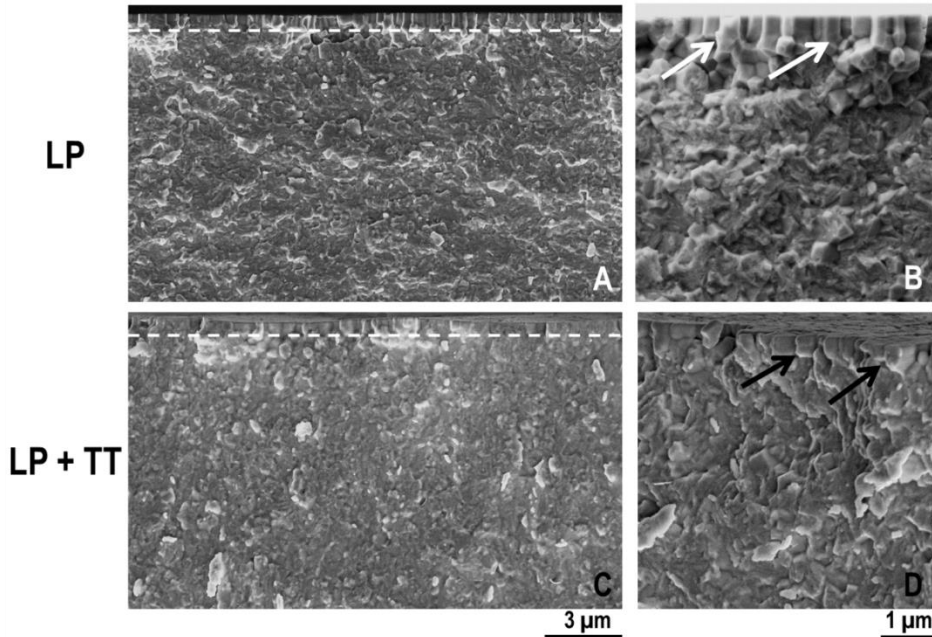

Fig.4. FESEM images of fracture surfaces of LP (A, B) and LP+TT (C,D) discs. In the higher magnification images (B, D) the distinction between the intergranular fracture layer (black and white arrows) from the transgranular fracture layer is more evident.

The intergranular fracture region corresponds to the thermally affected volume during laser treatment [87]. In this volume, fracture propagates along the pre-existing microcracks net on the surface (Fig 4B, D). Comparing LP to LP+TT fracture surfaces, it is interesting to note that the aspect of the grains in the intergranular fracture region is different: in LP samples, the corners of columnar grains are sharp while in LP+TT samples they are rounded and less defined.

3.2. Nanoindentation and scratch test

The integrity of laser treated surfaces was assessed with nanoindentation tests, evaluating the evolution of Hardness and Young Modulus as a function of indenter penetration. Laser patterned samples (LP and LP+TT) were compared to not treated 3Y-TZP (NT). Results are reported in Fig. 5.
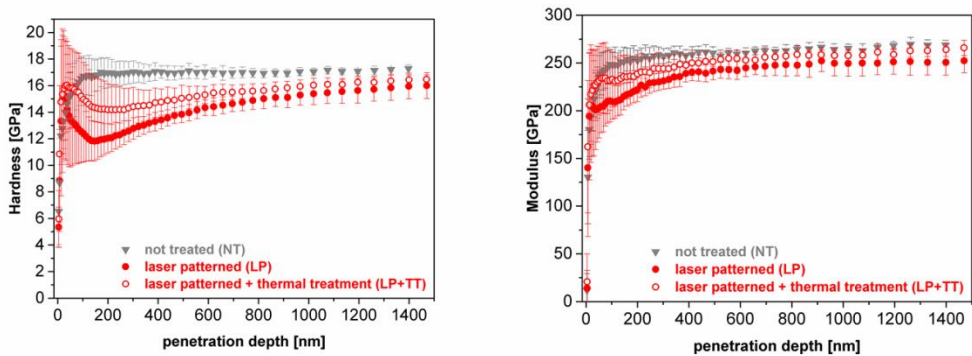
Fig. 5. Nanoindentation tests results of not treated (NT, grey triangles) and laser patterned before (LP, hollow red circles) and after thermal treatment (LP+TT, red circles) samples. In (A) the Hardness and in (B) the Young Modulus are plotted versus the indenter penetration depth.

For the not treated material a constant value of 17 GPa of Hardness and 250 GPa of Young Modulus can be defined after 150 nm of indenter penetration, compatibly with values reported typically in the literature for 3Y-TZP [98]. LP and LP+TT samples show a slight decrease both in Hardness and Young Modulus, which are recovered as the indenter penetrates further in depth of the laser treated surfaces. This loss can be related to the microcracked surface and the altered microstructure (elongated grains and $t \rightarrow m$ phase transformation) due to thermal effects caused by laser treatment [99,100] as well as the induced topography of the sample. No substantial difference can be observed between LP and LP+TT samples.

The scratch test performed provide a qualitative evaluation of the resistance to shear and friction of the laser patterned samples compared to a not treated surface of 3Y-TZP.
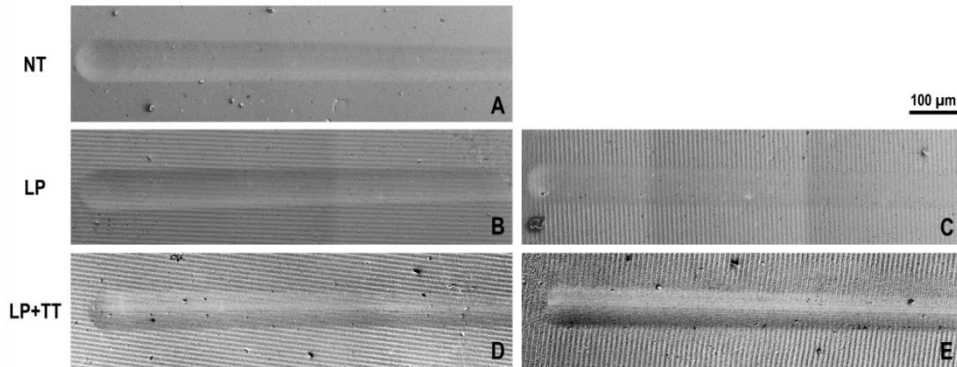

Fig.6. FESEM images of the scratches on not treated (A) and laser patterned before (B, C) and after (D, E) the thermal treatment. The relative orientation of pattern stripes and scratch direction is parallel in B and D and orthogonal in C and E.

In Fig.6 it is possible to observe that the scratches have similar sizes for all kind of samples. For the chosen parameters no fracture and material spallation occur, only a permanent plastic deformation in the wake below the indenter tip. No substantial difference can be observed between not treated (NT) and laser patterned samples before (LP) and after (LP+TT) thermal treatment, a part from the presence of cone cracks in the scratch on NT samples only. It is interesting to observe that the striped topography produced by laser is still appreciable inside the scratch wake. Furthermore, the direction of the scratch relative to pattern lines orientation seems not to be significant, showing an isotropic behavior.

4. Discussion

4.1. Mechanical properties and critical defects

From the obtained results, laser patterning seems to be at the origin of a slight decrease in the mechanical properties of 3Y-TZP. On the other hand, the thermal treatment seems not to affect the mechanical properties of the laser patterned samples. The biaxial strength of LP and LP+TT samples measured with B3B method is lowered while the Weibull modulus in increased (see Table 1 and Fig. 1). These features in the distribution may suggest a change in the population of critical defects, since the distribution

for LP and LP+TT samples is less scattered and shifted towards lower values of σ_f when compared to not treated 3Y-TZP (Fig. 1). In the following paragraph we will discuss how the laser treatment may affect defect population.

In a previous work [87] we have shown how laser patterning with ns-pulsed laser affects the microstructure of 3Y-TZP. Main modifications are concentrated in the first μm below the treated surface and have thermal origin. Microcracking, recrystallization, $t \rightarrow m$ phase transformation, t-phase texturization and residual stresses are the main consequences of the thermal shock produced during laser treatment. The presence of m-phase and residual stresses should not be responsible of the decrease in mechanical properties, since there is no difference in the biaxial strength and Weibull modulus in laser treated samples before (LP) and after the thermal treatment (LP+TT). In fact, annealing at 1200°C for 1h is able to relief residual stresses and revert m-phase to t-phase [91]. We are then left with a microcracked surface layer composed of columnar grains with a maximum thickness of 1 μm [87], corresponding to the intergranular fracture layer observed in the fractographic images (see Fig. 3). To understand if the decrease of strength is caused by this affected layer of material, a simple model is proposed. The microcracked surface layer is modeled as a straight through edge crack of thickness a. Then, the stress intensity factor K_I for the applied stress σ_{app} would be:

$$K_I = Y \, \sigma_{app} \sqrt{\pi a} \tag{5}$$

The geometric factor Y is 1.12 for this defect geometry [101]. Knowledge of the fracture toughness of the material is needed to determine a. For 3Y-TZP the values reported in the literature are scattered, depending on the method employed for its determination, because of the transformation toughening phenomenon and the nanometric grain size of 3Y-TZP. In this study we employed a value of $K_{IC} = 4.1$ MPa m$^{1/2}$ [102]. Considering $\sigma_{app\ LP} = \sigma_{o\ LP} = 1228$ MPa and $\sigma_{app\ LP+TT} = \sigma_{o\ LP+TT} = 1199$ MPa, the thickness of the affected layer acting as critical defect then should be $a_{LP} = 2.8$ μm and $a_{LP+TT} = 3.0$ μm for laser patterned samples before and after the thermal treatment, respectively. Since the laser affected layer reaches a maximum depth of 1 μm, the damage produced by laser alone cannot be at the origin of the fractures. This is in accordance with fractographic observations (Fig. 3): all the identified critical defects are porosities and low-density regions that most

probably are produced during processing and sintering steps. If this were the case, the critical defect can be modeled as circular surface crack of radius a. Then, the geometric factor Y would become 0.9 and the radius of the circular critical defect calculated with (5) would be a_{LP} = 4.4 µm and a_{LP+TT} = 4.7 µm, respectively. These values are in accordance with the experimental observations and the critical defects identified (Fig 2C and Fig. 3).

This kind of processing defects close to the surface have been identified as the most conventional cause of failure in 3Y-TZP [103]. However, there have to be some kind of influence of the laser treatment on the defect population that causes the observed change in Weibull distribution of failures (Fig. 1). Looking in more detail at some of the critical defects observed during fractography of a LP sample, it is possible to observe that the pre-existing defect (like a pore) may have been modified by the laser treatment.
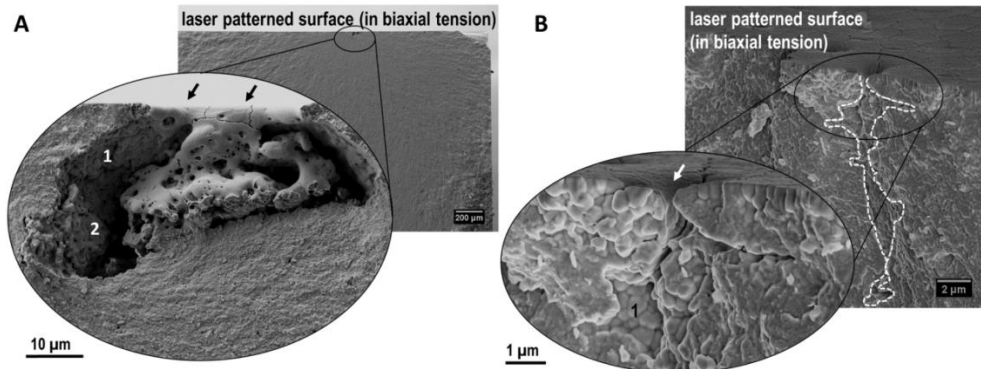

Fig. 7. FESEM magnification of critical defects showing the interaction of laser melting with pre-existing defects of the material. (A) LP sample (σ_f = 869 MPa) with a big pore on the surface: the inner walls of the pore have rounded grains (1) typical of sintering step but also show molten and resolidified material (2) typical of laser-induced melting. There is a molten rim on the laser treated surface (indicated by black arrows). (B) LP+TT sample (σ_f = 1208 MPa) with an elongated pore on the surface: the inner walls of the pore have rounded grains (1) typical of sintering step and there is a molten rim (indicated by white arrow) opening the pore to the surface.

In fig. 7A, a LP sample (discarded from Weibull analysis because fracture origin was at the periphery of the disc) has a big pore with the walls covered of rounded grains plus molten and resolidified material. There is a molten rim on the laser-treated surface (indicated by black arrows) and some partially molten material in the middle of the pore, as if the top of the defect has collapsed due to material melting. Similar observation can be done on a LP+TT sample (Fig. 7B): the elongated pore is opened to the surface by material melting (see again the presence of a molten rim indicated by the white arrow). Therefore it is possible that material melting on the surface

caused by the laser pulse may interact with defects already present inside the material (on the surface or right below it). Laser induced melting would result in the enlargement of preexisting defects. This would be compatible with the observed reduction in the Weibull characteristic strength observed after laser treatment (Table 1): the circular critical defect for not treated 3Y-TZP is 3.4 µm and becomes 4.4 µm after laser patterning. This effect could also be more pronounced in terms of strength reduction for defects very close to the surface that after laser treatment would become open to the surface, while melting of pre-existing open porosity may not have a significant effect.

It has been observed that in dielectrics the presence of preexisting defects on the surface (for instance absorbing impurities, cracks or rough cavities) could modify the normal laser absorption characteristics of the surface [104,105]. In fact, those defects can enhance laser absorption and therefore local material melting. Furthermore, if the defect has a lower heat transmission coefficient than the matrix (a pore filled with air in zirconia), the defect could also act as a thermal barrier causing local overheating [45]. These observations may be valid for 3Y-TZP and corroborate the hypothesis of defect enlargement due to material melting during laser exposure.

4.2. Surface integrity

Nanoindentation results show that the Hardness and Young modulus of the surfaces of 3Y-TZP decrease after the laser patterning (Fig. 5). The decrease in properties remains the same after the thermal treatment. Likewise discussed in previous paragraph about mechanical properties, microcracking then should be at the origin of this decrease in surface properties.

On the other hand, the laser affected layer seems not to strongly affect the integrity of the surface upon scratch (Fig. 6). In LP and LP+TT samples the damage produced by the spherical indenter does not compromise surface integrity more than in NT samples. Cone cracks are appreciated in the NT sample, typical of a brittle material [106]. This type of cracking cannot be appreciated in the LT materials. This can be attributed to the fact that the surface microcracks accommodate the deformation at the surface of the sliding contact, hindering, consequently, the formation of such cone cracks.

5. Conclusions

Laser patterning with DLIP induces a minor decrease in mechanical properties and surface integrity of 3Y-TZP. The biaxial strength (B3B) and the Hardness and Young modulus of the treated surfaces decrease as a consequence of the damage induced by laser patterning. Laser-affected layer could not be at the origin of fractures alone since its thickness is only 1 μm, well below the critical defect size. Laser interaction with pre-existing defects close to the surface result in an enlargement of such surface defects, thanks to focalization of laser radiation and subsequent material melting and damage. We believe that those enlarged critical defects are at the origin of the decrease in Weibull characteristic strength and the increase in Weibull modulus, as supported by the calculations of the critical defect size.

A thermal treatment after laser patterning does not alter further surface integrity and mechanical properties of laser patterned 3Y-TZP.

References

[1]   Implants for surgery — Ceramic materials based on yttria-stabilized tetragonal zirconia (Y-TZP) - EN ISO 13356:2013, (2013).

[2]   R.-J. Kohal, W. Att, M. Bächle, F. Butz, Ceramic abutments and ceramic oral implants . An update, Periodontol. 2000. 47 (2008) 224–243.

[3]   L. Treccani, T. Yvonne Klein, F. Meder, K. Pardun, K. Rezwan, Functionalized ceramics for biomedical, biotechnological and environmental applications., Acta Biomater. 9 (2013) 7115–50. doi:10.1016/j.actbio.2013.03.036.

[4]   Y. Ito, Surface micropatterning to regulate cell functions., Biomaterials. 20 (1999) 2333–42. http://www.ncbi.nlm.nih.gov/pubmed/10614939.

[5]   M.G. Holthaus, L. Treccani, K. Rezwan, Comparison of micropatterning methods for ceramic surfaces, J. Eur. Ceram. Soc. 31 (2011) 2809–2817. doi:10.1016/j.jeurceramsoc.2011.07.020.

[6]   M.G. Holthaus, S. Twardy, J. Stolle, O. Riemer, L. Treccani, E. Brinksmeier, K. Rezwan, Micromachining of ceramic surfaces: Hydroxyapatite and zirconia, J. Mater. Process. Technol. 212 (2012) 614–624. doi:10.1016/j.jmatprotec.2011.06.007.

[7]   A.N. Samant, N.B. Dahotre, Laser machining of structural ceramics—A review, J. Eur. Ceram. Soc. 29 (2009) 969–993. doi:10.1016/j.jeurceramsoc.2008.11.010.

[8]   A. Kurella, N.B. Dahotre, Review paper: surface modification for bioimplants: the role of laser surface engineering., J. Biomater. Appl. 20 (2005) 5–50. doi:10.1177/0885328205052974.

[9]   E. Roitero, F. Lasserre, M. Anglada, F. Mücklich, E. Jiménez-Piqué, A parametric study of laser interference surface patterning of dental zirconia: Effects of laser parameters on topography and surface quality, Dent. Mater. (2016) 10–14. doi:10.1016/j.dental.2016.09.040.

[10]   W.D. Kingery, H.K. Bowen, D.R. Uhlmann, Introduction to ceramics, second, 1976.

[11]   E. Roitero, F. Lasserre, J.J. Roa, M. Anglada, F. Mücklich, E. Jiménez-Piqué, Nanosecond-laser patterning of 3Y-TZP: Damage and microstructural changes, J. Eur. Ceram. Soc. 37 (2017) 4876–4887. doi:10.1016/j.jeurceramsoc.2017.05.052.

[12]   R. Danzer, A general strength distribution function for brittle materials, J. Eur. Ceram. Soc. 10 (1992) 461–472. doi:10.1016/0955-2219(92)90021-5.

[13]   C. Daniel, J. Drummond, R.A. Giordano, Improving Flexural Strength of Dental Restorative Ceramics Using Laser Interference Direct Structuring, J. Am. Ceram. Soc. 91 (2008) 3455–3457. doi:10.1111/j.1551-2916.2008.02642.x.

[14]   P.P. Shukla, J. Lawrence, Characterization and compositional study of a ZrO2 engineering ceramic irradiated with a fibre laser beam, Opt. Laser Technol. 43 (2011) 1292–1300. doi:10.1016/j.optlastec.2011.03.026.

[15]   B.S. Yilbas, Laser treatment of zirconia surface for improved surface hydrophobicity, J. Alloys Compd. 625 (2015) 208–215. doi:10.1016/j.jallcom.2014.11.069.

[16]   E. Roitero, M. Ochoa, M. Anglada, F. Mücklich, E. Jiménez-Piqué, Low temperature degradation of laser patterned 3Y-TZP:

Enhancement of resistance after thermal treatment, J. Eur. Ceram. Soc. (in press). doi:10.1016/j.jeurceramsoc.2017.10.044.

[17]   C. Daniel, F. Mücklich, Z. Liu, Periodical micro-nano-structuring of metallic surfaces by interfering laser beams, Appl. Surf. Sci. 208-209 (2003) 317–321. doi:10.1016/S0169-4332(02)01381-8.

[18]   M. Hans, C. Gachot, F. Müller, F. Mücklich, Direct laser interference structuring as a tool to gradually tune the wetting response of titanium and polyimide surfaces, Adv. Eng. Mater. 11 (2009) 795–800. doi:10.1002/adem.200900115.

[19]   R. Danzer, W. Harrer, P. Supancic, T. Lube, Z. Wang, A. B??rger, The ball on three balls test-Strength and failure analysis of different materials, J. Eur. Ceram. Soc. 27 (2007) 1481–1485. doi:10.1016/j.jeurceramsoc.2006.05.034.

[20]   A. Börger, P. Supancic, R. Danzer, The ball on three balls test for strength testing of brittle discs: stress distribution in the disc, J. Eur. Ceram. Soc. 22 (2002) 1425–1436. doi:10.1016/S0955-2219(01)00458-7.

[21]   W. Weibull, A statistical distribution function of wide applicability, J. Appl. Mech. 18 (1951) 293–297. doi:citeulike-article-id:8491543.

[22]   D. Munz, T. Fett, Ceramics : mechanical properties, failure behaviour, materials selection, Springer, 1999. doi:10.1007/978-3-642-33848-9.

[23]   W.C. Oliver, G.M. Pharr, Measurement of hardness and elastic modulus by instrumented indentation: Advances in understanding and refinements to methodology, J. Mater. Res. 19 (2004) 3–20. doi:10.1557/jmr.2004.19.1.3.

[24]   Y. Gaillard, M. Anglada, E. Jiménez-Piqué, Nanoindentation of yttria-doped zirconia: Effect of crystallographic structure on deformation mechanisms, J. Mater. Res. 24 (2009) 719–727. doi:10.1557/jmr.2009.0091.

[25]   Y. Gaillard, E. Jiménez-Piqué, F. Soldera, F. Mücklich, M. Anglada, Quantification of hydrothermal degradation in zirconia by nanoindentation, Acta Mater. 56 (2008) 4206–4216. doi:10.1016/j.actamat.2008.04.050.

[26]   A.C. Fischer-Cripps, A review of analysis methods for sub-micron indentation testing ⚙, Vacuum. 58 (2000) 569–585.

[27]   R. Danzer, On the relationship between ceramic strength and the requirements for mechanical design, J. Eur. Ceram. Soc. 34 (2014) 3435–3460. doi:10.1016/j.jeurceramsoc.2014.04.026.

[28]   M. Turon-Vinas, M. Anglada, Fracture toughness of zirconia from a shallow notch produced by ultra-short pulsed laser ablation, J. Eur. Ceram. Soc. 34 (2014) 3865–3870. doi:10.1016/j.jeurceramsoc.2014.05.009.

[29]   K. Noguchi, M. Fujita, T. Masaki, M. Mizushina, Tensile Strength of Yttria-Stabilized Tetragonal Zirconia Polycrystals, J. Am. Ceram. Soc. 72 (1989) 1305–1307. doi:10.1111/j.1151-2916.1989.tb09736.x.

[30]   S.G. Demos, M. Staggs, M.R. Kozlowski, Investigation of processes leading to damage growth in optical materials for large-aperture lasers., Appl. Opt. 41 (2002) 3628–3633. doi:10.1364/AO.41.003628.

[31]   H. Bercegol, P. Grua, D. Hebert, J.P. Morreeuw, Progress in the understanding of fracture related laser damage of fused silica - art. no. 672003, Laser-Induced Damage Opt. Mater. 2007. 6720 (2008) 72003. doi:10.1117/12.752830.

[32]   W.M. Steen, Laser material processing, 3rd ed, Springer, 2003.

[33]   L. Ceseracciu, M. Anglada, E. Jiménez-Piqué, Hertzian cone crack propagation on polycrystalline materials: Role of R-curve and residual stresses, Acta Mater. 56 (2008) 265–273. doi:10.1016/j.actamat.2007.09.030.

Acknowledgements

Prof. Emilio Jiménez-Piqué, my supervisor at UPC. My sincere gratitude for the guidance, confidence and support during my entire PhD. Your curiosity and passion for science are admirable. I learned a lot about hard materials and nanomechanics and to see technical problems and scientific doubts as a constructive purpose.

Prof. Frank Mücklich, my supervisor at UDS. Thank you for giving me the opportunity of being part of your research group and letting me work in the laser facilities. I have learned a lot during my internships in Saarbrücken.

All the members of *CIEFMA group* at UPC. Thank you for the warm welcome from the very first day and for sharing your expertise on hard materials and mechanical characterization. Special thanks to *Prof. Marc Anglada* for giving me the opportunity of being part of your research group and sharing your extensive knowledge on zirconia ceramics. *Prof. Joan Josep Roa*, thanks for your assistance and availability. *Fernando*, thanks for your patience in teaching me how to deal with so many "rebel" machines in the CMEM labs...and to *Kim*, for being able of fixing all of them! *Dr. Erik Camposilvan* and *Dr. Quentin Flamant*, my gratitude to you for sharing your precious experience and for introducing me to dental zirconia...by singing! You are the funniest "PhD mentors" one could have. *Almost-Dr. Miquel Turon Viñas*, this thesis would have been very different (i.e., really crappy) without your precious graphic competence and ability to trick Word bugs...you are the most patient office mate ever! An acknowledgement to the students who did their master project with me, especially *Miguel Ochoa*, *Victoria Gonzalez* and *Adrian Bouzo*. Also thanks to *Dr. José Alejandro Muñoz Tabares*, even if I did not have the chance to meet you in person I learned so much about zirconia microstructure from your thesis (I read it so many times that it is almost worn out).

All the members of *CRnE* (now Multiscale). Thank you for giving me the opportunity to work "hands on" all the facilities in your nice laboratories, I learned a lot about practical scientific work. Special thanks to *Trifon*, the FIB-SEM wizard, for the immense patience in teaching me how to dig a micrometric trench. Thanks *Montse* for your patience and competence and for being always available.

All the members of *FUWE group* at UDS. Thank you for teaching me how to work with a "big scary laser" without losing an eye. Thanks a lot for your availability and patience to answer to all my questions and doubts one and another time. Special thanks go to *Federico Lasserre*, who is the best (and fastest) coauthor ever, and to *Dr. Sebastian Suarez* and *Jenifer Barrirero* for working with me and helping so much with the delicate topic of TEM lamellas.

Erasmus Mundus Joint Doctoral Programme (DocMASE). My gratitude goes to the DocMASE programme and the Erasmus Mundus scholarship for funding my PhD studies and allowing me to live such a great international research experience. Very special thanks go to *Flavio Soldera*, for his commitment and patience.

Irene Perez. Thanks for guiding me through the intricate labyrinth of bureaucracy and co-tutorship agreements.

Reviewers. Sincere gratitude to the unknown reviewers who took the time to read my manuscripts and with their corrections helped me to improve my work.

Here end the official and formal acknowledgments: all these people and institutions contributed substantially to my scientific skills and knowledge. However, a part from the scientific work, the big challenge of the PhD to me was to maintain balance and to carry on a 4-years-project, trying to keep high the motivation (or at least not freak out and quit). I was so lucky to have many people with whom to share the ups and downs of life: thank you for accepting me, for listening and making me smile.

Mi *jefe Emilio*. Gracias por enseñarme este oficio que es la investigación de manera siempre muy humilde y humana. Has sido un guía de gran sensibilidad y paciencia infinita. Gracias por confiar en mis capacidades, sobre todo cuando yo ya no lo hacía...aun no sé cómo lograste a hacerme escribir el primer paper! Eres mi scientific jedi master.

Los *Pollitos*: *Berni, las Danielas (es broma...Dani T. y Dani S.), Erik, Giuseppe, Ina, Jing, Jose Maria, Mireia, Miquel, Quentin, Romain y su divertido amigo John Gall Speed, Roberta (mi querida compis) y Yassine.* Un agradecimiento especial a este grupo de gente increíble que me ha acompañado de cerca durante esta larga aventura del doctorado: hemos compartido el día a día del trabajo, los muffins de chocolate (partidos en n! trozos) y divertidísimas actividades extracurriculares. Nunca me sentí sola: